

# UC San Diego

## UC San Diego Electronic Theses and Dissertations

### Title

Post-Mitotic Reformation of the Nuclear Envelope and Aberrant Nuclear Envelope Rupturing During Interphase in Human Cancer Cells.

### Permalink

<https://escholarship.org/uc/item/3h52g6xp>

### Author

Vargas, Jesse

### Publication Date

2012

### Supplemental Material

<https://escholarship.org/uc/item/3h52g6xp#supplemental>

Peer reviewed|Thesis/dissertation

UNIVERSITY OF CALIFORNIA, SAN DIEGO

**Post-Mitotic Reformation of the Nuclear Envelope and Aberrant Nuclear  
Envelope Rupturing During Interphase in Human Cancer Cells.**

A dissertation submitted in partial satisfaction of the requirements for the  
degree

Doctor of Philosophy

in

Biology

by

Jesse Vargas

Committee in charge:

Professor Martin W. Hetzer, Chair  
Professor Arshad B. Desai  
Professor William McGinnis  
Professor Clodagh C. O'Shea  
Professor Lorraine Pillus

2012

Copyright

Jesse Vargas, 2012

All rights reserved.

The Dissertation of Jesse Vargas is approved, and it is acceptable in quality and form for publication on microfilm and electronically:

---

---

---

---

---

Chair

University of California, San Diego

2012

## DEDICATION

This thesis is dedicated to a dream unrealized, the dream of countless students across the nation who, without economic means, find it increasingly difficult if not impossible to pursue higher education, a college degree, and to follow their own academic pursuits; and to hope for change and greater access to opportunity in the future. A great deal of luck, along with the repeated generosity of both family and total strangers, contributed in immeasurable ways, to the endeavor culminated herein.

## TABLE OF CONTENTS

Signature Page .....	iii
Dedication .....	iv
Table of Contents .....	v
List of Figures .....	x
List of Tables .....	xii
List of Abbreviations .....	xiii
Acknowledgements .....	xiv
Vita .....	xviii
Abstract of the Dissertation.....	xxi
<b>Chapter I Introduction .....</b>	<b>1</b>
Introduction: The nucleus, where the genome meets cell biology.....	2
Nuclear Envelope Structure .....	3
Nuclear Envelope and Mitosis.....	5
Nuclear Envelope Breakdown and Reformation .....	6
Nuclear Envelope and Disease .....	7
Aberrant Nuclear Morphology in Cancer.....	9
Summary .....	11
Acknowledgments.....	11

<b>Chapter II Recruitment of functionally distinct membrane proteins to chromatin mediates nuclear envelope formation in vivo .....</b>	<b>18</b>
Abstract.....	19
Introduction .....	20
Results .....	21
Measuring NE formation in vivo .....	21
Reduced levels of INM proteins limit the rate of NE formation.....	22
Functionally distinct chromatin-interacting proteins mediate NE formation .....	23
Reduction of BAF, Lap2 $\beta$ , or Ndc1 delays final stages of NE formation .....	24
INM proteins are positive regulators of NE formation.....	25
Nuclear targeting of Lap2 $\beta$ is independent of expression level.....	27
Tethering of membranes to chromatin is required for NE formation acceleration.....	28
Accelerating NE formation decreases chromosome separation during mitosis .....	29
Conclusion .....	30
Methods .....	32
Acknowledgements.....	36

<b>Chapter III Transient nuclear envelope rupturing during interphase in human cancer cells .....</b>	<b>52</b>
Abstract.....	53
Introduction .....	54
Results.....	57
Transient mislocalization of nuclear GFP <sub>3</sub> -NLS in cancer cells .....	57
Knockdown of lamins increases the frequency of NE rupturing during interphase.....	60
Interphase NE rupturing causes mislocalization of cellular components .....	64
NE rupturing causes temporary loss of cellular compartmentalization.	67
Discussion.....	69
Materials and Methods .....	74
Acknowledgments.....	79

<b>Chapter IV Conclusion .....</b>	<b>96</b>
<b>DNA/chromatin interacting membrane proteins of the INM role in</b>	
<b>post-mitotic reformation of the NE.....</b>	<b>97</b>
Key findings of Chapter II .....	98
Functionally distinct proteins are co-opted for NE formation at the	
conclusion of mitosis .....	98
Aggregate expression level of membrane-chromatin tethering	
proteins controls the rate of post-mitotic NE formation .....	99
Regulation of NE formation timing is critical for proper cell division	
processes.....	100
A fundamental step of cellular division can be accelerated by	
altering gene expression level.....	100
<b>NERDI: characterization of a previously unknown phenomenon in</b>	
<b>human cancer cells .....</b>	<b>101</b>
Key findings of Chapter III .....	103
Nuclei of several commonly used human cancer cell lines	
transiently rupture during interphase .....	103
Frequency of interphase rupture is linked to the expression level of	
structural proteins of the NE .....	104
Nuclear ruptures are bidirectional with mislocalization of nuclear	
and cytoplasmic proteins.....	104

Nuclear ruptures may impart significant genomic insult and contribute to the mutation capacity of cancer cells.....	106
<b>Acknowledgements</b> .....	106
<b>References</b> .....	109

## LIST OF FIGURES

### Chapter I

Chapter I Figure 1: Schematic drawing of the mammalian nucleus structure and connections to the cytoskeleton .....	12
Chapter I Figure 2: TEM of HeLa cell indicating nuclear and cytoplasmic spaces .....	14
Chapter I Figure 3: Life cycle of the metazoan cell .....	16

### Chapter II

Chapter II Figure 1: Chromatin-binding NE proteins collaborate during NE Formation .....	37
Chapter II Figure 2: Chromatin-interacting NE proteins promote nuclear assembly .....	39
Chapter II Figure 3: Membrane-chromatin tethering function of Lap2 $\beta$ in NE formation .....	41
Chapter II Figure 4: Acceleration of nuclear membrane formation causes chromosome segregation defect .....	43
Chapter II Supplemental Figure 1: Reduction of chromatin-binding proteins delays accumulation of membranes at the chromatin surface during NE formation .....	45
Chapter II Supplemental Figure 2: Localization of V5-tagged constructs ....	47

### Chapter III

Chapter III Figure 1: Nuclear envelope rupture during interphase .....	81
Chapter III Figure 2: Reduced lamin levels accentuate nuclear ruptures ....	83

Chapter III Figure 3: Mislocalization of nuclear and cytoplasmic components .....	85
Chapter III Figure 4: Consequences of interphase nuclear rupture .....	87
Chapter III Supplemental Figure 1: GFP <sub>3</sub> -NLS expression & localization .....	89
Chapter III Supplemental Figure 2: Lamin knock down and differential expression .....	91
Chapter III Supplemental Figure 3: shRNA stable lamin knock down .....	93
Chapter IV	
Chapter IV Figure 1: Inhibiting NERDI reduces DNA damage staining .....	107

## LIST OF TABLES

### Chapter III

Chapter II Table S1: Average NEF times and statistics for siRNA-mediated knockdown of selected proteins .....	49
Chapter II Table S2: Average NEF times and statistics for transiently increased expression levels of selected proteins .....	50
Chapter II Table S3: Average NEF times and statistics for combination siRNA and kinetic rescue experiments .....	51

## LIST OF ABBREVIATIONS

Abbreviation	Definition
~	approximately
>	greater than
<	less than
BAF	barrier to autointegration factor
DNA	Deoxyribonucleic acid
EM	electron microscopy
ER	endoplasmic reticulum
GFP	green fluorescent protein
HeLa	cell line derived from cervical cancer
HP1	heterochromatin Protein 1
INM	inner nuclear membrane
LINC	linker of nucleus and cytoskeleton
NE	nuclear envelope
NEBD	nuclear envelope breakdown
NEF	nuclear envelope formation
NERDI	nuclear envelope rupturing during interphase
NLS	nuclear localization signal
NPC	nuclear pore complex
Nup	nucleoporin
ONM	outer nuclear membrane
PCR	polymerase chain reaction
RNA	ribonucleic acid
Rtn	Reticulon
siRNA	small interfering RNA
SJSA	human osteosarcoma cell line
tdTomato	tandem-dimer Tomato
TEM	transmission electron microscopy
U2OS	human osteosarcoma cell line

## ACKNOWLEDGEMENTS

Serendipity, it seems, saw it fit to set me in a room to hear an up and coming Associate Professor from the Salk Institute give a dynamic talk about his work during the first week of my PhD at UCSD. Several months later I found myself immersed in a rotation project in his innovative lab. That work would become the first publication of my PhD, and the Associate Professor, Martin W. Hetzer, would, over the course of the next several years, guide me through my dissertation research. Along the way, Martin would rise through the ranks at the Salk to Professor, Jesse and Caryl Phillips Foundation Chair, and Faculty Director of The Waitt Advanced Biophotonics Center; and his passion for microscopy and brilliance in investigative scientific research would shape the course of my education. The breathtaking pace and productivity of his lab would, but for my own personal experience with experimental setbacks, beguile his patience and ability to maintain a close working relationship with, and genuine concern for the researchers he mentors. I would like to express my appreciation and respect for Martin and the science done in his lab. My committee: Bill McGinnis, Lorraine Pillus, Clodagh O'Shea, and Arshad Desai, have all been supportive and truly interested in my PhD education and thesis work. They have pushed me to ask the right questions and, in so doing, have made me a better scientist and for that I am indebted and grateful.

The members of the Hetzer lab have been helpful and supportive; my day-to-day companions with whom I have spent the majority of the last 4 years of my life. Their insight, expertise, and general camaraderie have made my PhD memorable and rewarding, and have helped to create for me what will surely be some of the memories I take with me for the rest of my life. For that and for many reasons too numerous to list, I thank them. I want to extend a special thanks to Daniel J. Anderson, a former graduate student that oversaw my initial training and introduction to advanced microscopy, and who I worked very closely with for 2 years. Dan's energy and enthusiasm started my tenure in the Hetzer lab off on an exciting and highly productive foot and I will be forever grateful for his continued friendship, advice and support. I would also like to thank the senior post-docs and the lab manager who were great resources of information, support and advice, Maximiliano D'Angelo, Maya Capelson, Christine Doucet, and Robbie Schulte, as well as the new post-docs and my fellow grad students in the lab for many things, but mostly for their continual laboratory entertainment. To Associate Dean of Education, Gabriele Wienhausen, for continued support and advocacy of graduate students and the general improvement of graduate student life at UCSD, my gratitude. It was a pleasure to work with you to improve student life and diverse representation.

I want to acknowledge my two sisters Maria Petrovski and Kelly Koleszar for their continuous support and encouragement, my two nephews

Will Rahn and Scott Rahn, and my twin nieces Aleksandra (Allie) Petrovski and Viktoria (Tori) Petrovski for keeping me optimistic and hopeful for the future.

Chapter 1, in full, is original text compiled from information in the primary literature and written in its entirety by Jesse D. Vargas.

Chapter 2, in full, consists of the following publication:

Anderson DJ\*, Vargas JD\*, Hsiao JP, and Hetzer MW. 2009.  
**Recruitment of functionally distinct membrane proteins to chromatin mediates nuclear envelope formation in vivo. JCB**  
186(2): 183-91; doi: 10.1083/jcb.200901106

(\* indicates co-first authorship)

© Anderson DJ, Vargas JD, Hsiao JP, Hetzer MW. 2009. **JCB**.

Daniel Anderson and I were the primary researchers and authors for these studies under the supervision and direction of Martin Hetzer. Joshua Hsiao performed a portion of the molecular cloning of constructs used in this study.

Chapter 3, in full, consists of the following publication:

Vargas JD, Hatch EM, Anderson DJ, Hetzer MW. 2012. **Transient nuclear envelope rupture during interphase in human cancer cells.**

**Nucleus** 3(1): 88-100; doi: 10.4161/nucl.3.1.18954

© Vargas JD, Hatch EM, Anderson DJ, Hetzer MW. 2012. **Nucleus.**

I was the primary researcher and author of these studies under the supervision and direction of Martin Hetzer. Emily Hatch contributed experimental work to this study. Daniel Anderson made initial observations, developed preliminary imaging assays and analysis methods for this study.

## VITA

### EDUCATION

- 2012                    **Ph.D., Biology**  
**Molecular and Cellular Biology**  
University of California, San Diego / Salk Institute  
San Diego, CA
- 2007                    **M.S., Molecular, Cellular & Systemic Physiology**  
Southern Illinois University, Carbondale  
Carbondale, IL
- 2003                    **B.S., Biological Sciences**  
University of California, Irvine  
Irvine, CA
- 2003                    **B.S., Chemistry**  
University of California, Irvine  
Irvine, CA
- 1996                    **High School Diploma**  
Barstow High School  
Barstow, CA

### WORK EXPERIENCE

- 2008-2012            Graduate Researcher, The Salk Institute
- 2005-2007            Graduate Researcher, So.IL University Carbondale
- 2002-2005            Advisor/Adjunct Instructor, University of CA, Irvine
- 2001-2004            Program Director, University of CA, Irvine
- 2001-2002            Mentor Tutor, University of CA, Irvine
- 1999-2001            Tutor, University of CA, Irvine
- 1994-1996            Tutor, Barstow Community College

## PUBLICATIONS

**Vargas JD**, Hatch EM, Anderson DJ, Hetzer MW. 2012. Transient nuclear envelope rupture during interphase in human cancer cells. *Nucleus* 3(1):88-100

Anderson DJ\*, **Vargas JD\***, Hsiao JP, Hetzer MW. 2009 Recruitment of functionally distinct membrane proteins to chromatin mediates nuclear envelope formation in vivo. *JCB* 186(2):183-91

(\* indicates co-first authorship)

Sparks SM, **Vargas JD**, Shea KJ 2000. Type 2 intramolecular nitroso Diels-Alder reaction. Synthesis and structure of bridgehead oxazinolactams. *Org. Lett.* 2(10):1473-5

## TEACHING AND MENTORSHIP

Teaching assistant for Dr. Steve Briggs, Advanced Bioinformatics Programming, University of California San Diego, Winter 2009.

Teaching assistant for Dr. James Ferraro, Mammalian Physiology Lab, Southern Illinois University, Carbondale, Fall 2006.

Mentor to rotation student Valentino Gantz, Winter 2009.

Mentor to rotation student Bessie Su, Spring 2009.

Adjunct Instructor, UC Irvine, Cell Biology 2004-5.

Adjunct Instructor, UC Irvine, Organic Chemistry 2003.

Program Director, CAMP Summer Science Academy UC Irvine 2002-4.

Tutor Advisor, UC Irvine, Division of Chemistry 2002-5.

Mentor Tutor, UC Irvine, Organic Chemistry 2000-2.

Mentor, CAMP Summer Science Academy 200-2.

## **FIELDS OF STUDY**

Major Field: **Biology**

### **Studies in Molecular and Cellular Biology**

Professor Martin W. Hetzer

The Salk Institute for Biological Studies

### **Studies in Molecular and Cellular Physiology**

Associate Professor Michael W. Collard

Southern Illinois University, Carbondale

### **Studies in Synthetic Organic Chemistry**

Professor Ken J. Shea

University of California, Irvine

## ABSTRACT OF THE DISSERTATION

Post-Mitotic Reformation of the Nuclear Envelope and Aberrant Nuclear  
Envelope Rupturing During Interphase in Human Cancer Cells.

by

Jesse Vargas

Doctor of Philosophy in Biology

University of California, San Diego, 2012

Professor Martin W. Hetzer, Chair

The nucleus, defined by its enclosing boundary, the nuclear envelope, is the largest organelle in most eukaryotic cells and houses the nuclear genome. It has been implicated in various physiological processes crucial to normal cell function, processes that are often altered in disease. Here we show that the re-establishment of this critical organelle after cellular division is achieved by a co-opting of numerous proteins of the inner nuclear membrane that interact with DNA/chromatin and that each serve distinct interphase functions. That such a large number of proteins and resources are dedicated to the rapid reformation of the nuclear envelope and proper nuclear compartmentalization suggests its critical importance for normal cell function.

Subsequently, we show that this barrier function and the integrity of the nuclear envelope is transiently disrupted in human cancer cells, leading to the mislocalization of both nuclear and cytoplasmic proteins. In extreme cases, this loss of integrity leads to a partial loss of cellular compartmentalization, with normally cytoplasmic organelles appearing in the interior of the cell nucleus. These rupture events are transient and recoverable, but the efflux of genomic material from the nucleus during such events suggests potential genomic insult that may contribute to alterations in genetic information and to the transformation process in cancer.

## CHAPTER I

### Introduction

**Introduction: The nucleus, where the genome meets cell biology.**

The nucleus is the most prominent feature of eukaryotic cells (Fig. 1 and 2) and the structure for which the domain Eukarya owes its name. The nucleus is defined by its outermost barrier, the nuclear envelope (NE), a double phospholipid membrane that completely encloses the nuclear genome and isolates it and its requisite genomic activity from the rest of the cell.<sup>1,2</sup> The nucleus was the first sub-cellular structure ever observed through a microscope, and was depicted in drawings of the microscopist Antoine van Leeuwenhoek in the early 1700s. By the late 1800s the nucleus was implicated as an important structure in the heredity system in cells and by the early 1900s the nucleus was demonstrated to be a regulated space within the cell.<sup>3</sup> It is now known that the nucleus serves as the primary repository for genetic information in the cell, and through its highly regulated spatial separation from the remainder of the cell, facilitates a number of physiologically relevant processes such as transcription, transcriptional regulation and the three-dimensional organization of the genome.<sup>4,5</sup> The nucleus and nuclear envelope have, after a lengthy period of being viewed as a static structure, seen a rebirth over the past few decades, with increasing scientific interest evidenced by an exponential increase in annual publications on nuclear structures, their basic cell biology, and links to complex phenomena such as differentiation, aging, and disease.<sup>6-8</sup> Indeed, the current

mammalian localization database places nearly 30% of known proteins in the nuclear space, with still other proteins interacting with the nucleus in some manner throughout the various biological processes of the cell. It is evident, with the rise in interest in the nucleus in terms of chromatin structure and genomic organization, and with implications of aberrant nuclear organization in genetic diseases and cancer, that the nucleus will continue to be an active area of research in the decades to come.

### **Nuclear Envelope Structure**

The NE is composed of a double phospholipid bilayer that is divided into 3 primary components: the outer nuclear membrane (ONM) which is studded with ribosomes and forms a continuous membrane system with the rough endoplasmic reticulum (ER); the inner nuclear membrane which hosts a distinct protein complement with proteins that interact with chromatin and the underlying nuclear lamina, the filamentous network thought to provide mechanical stiffness and structural support to the delicate phospholipid envelope; and the perinuclear space that separates the outer and inner membranes by a space of between 10 and 50 nm and is continuous with the lumen of the ER.<sup>3,1,9-12,2</sup>

The ONM and INM of the NE is fused at points where it is fenestrated by large multi-protein complexes responsible for regulating macro-molecular

traffic into and out of the nucleus. These nuclear pore complexes (NPCs) are composed of approximately 30 different proteins called nucleoporins (Nups) that are present in multiples of 8 in a ring like structure that forms a central aqueous transport channel through the hydrophobic lipids of the dual NE membranes. The multiplicity of the Nups in the NPC produces an 8-fold radial symmetry readily apparent in surface images taken by electron microscopy (EM).<sup>13</sup> On their cytoplasmic face, NPCs exhibit a series of amorphous phenylalanine-glycine repeats thought to provide the permeability barrier of the pore and to be important for interaction with transport cargo receptors such as the karyopherin family of importins.<sup>14,15</sup> On their nuclear face, NPCs are characterized by the presence of a nuclear basket, a structure of filamentous protein threads terminating in a final protein ring structure at their most nuclear-interior extreme. In addition to their transport channel forming function, the Nups are also thought to stabilize the highly curved “pore membrane” that results from the fusion of INM and ONM at their sites of insertion.

The fairly uniform spacing of the INM and ONM results from the luminal interaction of two classes of nuclear membrane proteins. The INM Sun proteins interact through their Sun domains with the KASH domains present in the ONM Nesprin family of proteins. In addition to the maintenance of proper membrane spacing, the Suns interact with the underlying nuclear lamina. The Nesprins interact with the cytoskeleton. Together the Suns and

Nesprins, together with the lamina and cytoskeleton form the so-termed LINC (linker of nucleus and cytoskeleton) complex that connects the nucleus to the cytoskeleton of the cell and has been implicated in cell motility and nuclear positioning.<sup>9-11</sup>

The underlying filamentous lamina is composed of type V intermediate filament proteins, the A and B type lamins. The A (lamin A and lamin C) type lamins are transcribed from a single gene as alternate splice variants and are developmentally expressed. The B (lamin B1 and B2) type lamins are expressed from individual genes and are thought to be expressed in all cells. Together, the lamins oligomerize into a mesh-like structure just beneath, and tightly connected to, the INM through protein-protein interactions. The composition of the various lamins in the lamina varies among different cell types and is thought to be linked with differential mechanical properties of the nuclei in these cell types (Fig.1).

### **Nuclear Envelope and Mitosis**

In metazoa, the highly regulated process of cell division during mitosis, with its concomitant partitioning of cellular organelles, proteins, and replicated copies of the genomes to each daughter cell, requires the breakdown of the nuclear envelope. It is thought that such breakdown allows for the complicated series of events necessary to properly align, form spindle

attachments to, and finally segregate sister chromatids to opposite poles of the cell during mitosis. Of course such an event requires the faithful reconstruction of the nucleus upon completion of each division cycle.

### **Nuclear Envelope Breakdown and Reformation**

During mitosis, the NE is broken down and retracted into the mitotic ER. In late prophase (pro-metaphase), a series of phosphorylation events lead to the rapid disassembly of the nuclear lamina, the underlying support structure of the NE, and the disassembly of the NPCs (Fig. 3).<sup>16-18</sup> The Nups are dispersed, along with the lamin proteins, throughout the mitotic cytoplasm. With the loss of these stabilizing protein structures, the membrane system of the NE is retracted into the mitotic ER, along with the resident proteins of the NE, where they will remain during the metaphase and anaphase portions of mitosis until the NE begins to reform in the late anaphase to telophase transition (Fig. 3).

Reformation of the NE involves a massive reorganization of the internal cellular membranes. Namely, the NE must re-emerge from the mitotic ER network to encapsulate the isolated chromosome clusters present in late anaphase. To achieve this, membrane-bending proteins of the ER must be displaced from the flattening membranes at the chromatin surface. As the NE reforms around the chromosome clusters that will become the daughter

nuclei, NPCs are re-assembled at the NE and will continue to be inserted throughout interphase to allow for sufficient nuclear transport capacity to be maintained from generation to generation (Fig. 3).<sup>19-21</sup>

Whether the re-emergence of the NE occurs primarily from the ER tubules or from the flatter ER cisternae sheets remains controversial, with studies showing an importance for the displacement of the reticulon family of ER tubule proteins and initial tubule-chromatin contact followed by later cisternae presence supporting the ER tubule source, and with 3D reconstruction studies showing primarily flat reticulon-free membranes proximal to chromatin masses during anaphase.<sup>22-25</sup> It is clear that more study in this area, namely involving high temporal and spatial resolution of dynamic membrane shaping and protein movements, will be needed to unequivocally resolve the question. While the exact structure of the membranes that contribute to NE reformation is not firmly known, it has been postulated that the driving force of membrane recruitment to chromatin is the DNA/chromatin interaction domains present in INM proteins of the NE that are stored in the ER during mitosis.

### **Nuclear Envelope and Disease**

Over the past several decades the cell nucleus has emerged as a critically important subcellular structure in human genetic disease. Mutations

in the proteins of the NE, the underlying nuclear lamin proteins, or the proteins that make up the connection between the nucleus and cytoskeleton have been implicated in a variety of human disease with moderate to severe effects on diverse tissues of the body, and in some cases on more general physiological processes such as development and aging. The most well studied of such diseases, perhaps owing to its striking clinical presentation, is the premature aging disorder, Progeria.

Progeria and progerid-like disorders manifest as a rapid onset of age-related phenotypes with afflicted individuals exhibiting infirmed characteristics in early childhood. The most common form of the disorder has been shown to result from a single mutation in the gene encoding lamin A. This mutation activates a cryptic splice site that causes a premature and unprocessed form of lamin A to be expressed in the cell. The lamin of afflicted individuals is uncharacteristically thickened and irregular in appearance.<sup>26-29</sup> Exactly how this aberrant lamin proteins contributes to the associated aging phenotype is not well understood, however, afflicted individuals commonly do not survive past their early to mid twenties, often succumbing to cardiac failure or stroke.

Other common disorders related to mutation of nuclear proteins include muscular dystrophies, such as the monogenic Emery-Dreyfus Muscular Dystrophy linked to mutations in the INM protein emerin and again to lamins, lipodystrophies linked to primarily lamin A, skeletal dysplasias

linked to INM proteins LBR and Man1, neurological disorders such as cerebellar ataxia linked to the nesprin SYNE1, and the dilated cardiomyopathies that are linked to various lamin mutations or to mutations in the INM protein Lap2 $\beta$ .<sup>6,30-34</sup> In all there are several subtypes of Emery-Dreyfus muscular dystrophies, as well other types of muscular dystrophy, such as limb-girdle disease, have been linked to the NE with, cardiomyopathy disorders and various lipodystrophies and neurological disorders also associated, making a strong argument for the complex and pleiotropic nature of NE protein function. Of clinical interest, the majority of phenotypes associated with NE related genetic disease impact structures and tissues under specific mechanical stress within the body, perhaps implicating the nucleus as a primary component of the cells ability to cope with force transduction through a tissue.

### **Aberrant Nuclear Morphology in Cancer**

Since the 1950's clinicians and pathologists have recognized a link between nuclear morphology and cancer. Indeed routine grading of tumors by pathology today still often includes an analysis of nuclear irregularity in shape, size, and uniformity of staining. While the cause of such irregularities is poorly understood, the indication for clinical prognosis is well established. Namely, aberrant nuclear morphology is associated with advanced stages of

cancer, poor prognosis and often metastatic transformation, the point at which many primary cancer lesions become a critical threat to patient survival.<sup>35-37</sup> Additionally, changes in nuclear localization have been associated with poor clinical outcome, and changes in NPCs and Nups have been linked to entry and exit from drug resistance dormancy.<sup>38-40</sup> While the nucleus has been used for circa ½ a century as a clinical indicator, only in the last few decades has an increasing focus on the nucleus in the area of cancer cell biology been realized. Several studies now have linked abnormal expression of nuclear proteins such as the nuclear lamins and nuclear proteins of the INM to cancer. Still others have linked changes in nuclear architecture, such as the 3D organization of the genome and changes in heterochromatin disposition, to cancer, increased metastatic potential, or lethality. While not as ubiquitous to neoplastic transformation as mutations in p53 or Rb protein, changes in nuclear proteins (INM and ONM proteins, Lamins, Nups, importins, etc.) have been described in cancers as diverse as those arising from the lung, gastrointestinal tract, skin, breast, ovaries, colorectal tissue, hepatocellular and blood, suggesting a likely commonality in many diverse types of cancer.<sup>39,41-45</sup>

## **Summary**

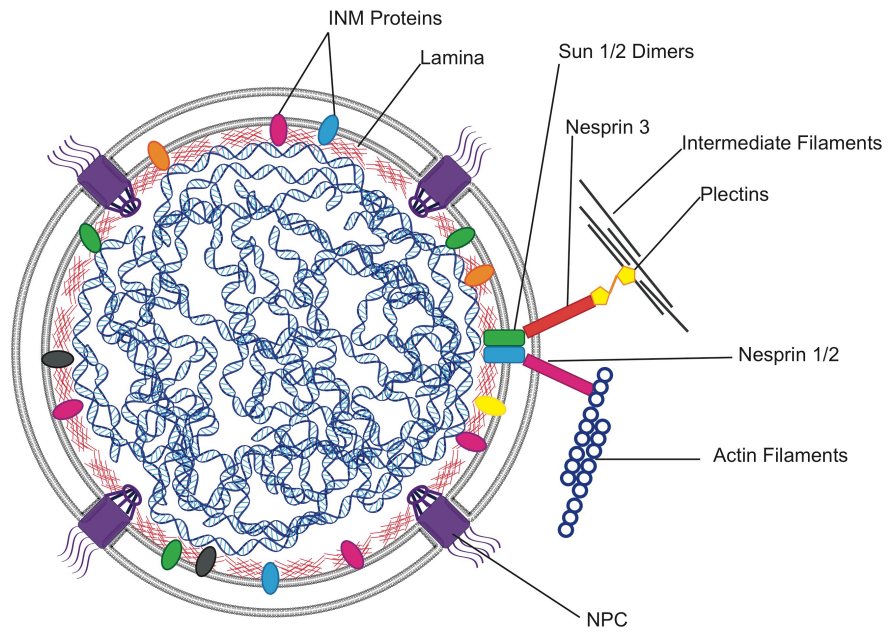
The nucleus is a complex organelle and organization center in eukaryotic cells. Through its various genome related roles it controls processes that determine cell fate decisions, response to transcription activating or repressing environmental cues, and maintenance of differentiation and cell identity state. Its interactions with the cytoskeleton makes it a key player in the dynamics of cell positioning, motility, and the general structural integrity and force transducing characteristics of the cell. Finally the barrier function of the nuclear membrane and the regulated transport through the embedded NPCs effectively compartmentalize nuclear function and likely provide a protective environment for the genome and genomic activity. It is clear the pleiotropic nature of nuclear function will continue to be an active area of continued interest, enhanced by emerging technologies in genome biology and imaging techniques attempting to push both live and fixed imaging beyond the diffraction limit of visible light that will enable studies to probe deeper and at a level of temporal and spatial detail previously unavailable.

## **Acknowledgements**

Chapter 1 is original text compiled from information in the primary literature and written in its entirety by Jesse Vargas.

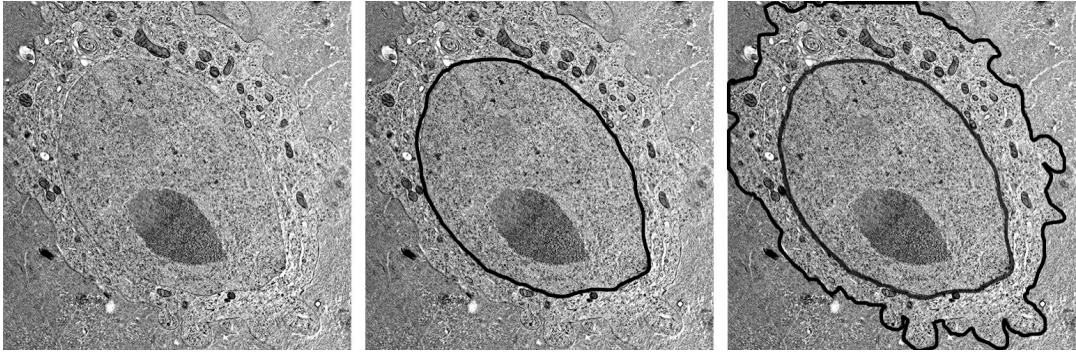
**Chapter I Figure 1: Schematic drawing of the mammalian nucleus structure and connections to the cytoskeleton.**

Schematic illustration of mammalian cell nucleus with encapsulating double phospholipid bilayer in black, underlying nuclear lamina in red, NPCs in purple, INM proteins in various colors, DNA/chromatin in dark blue, and the proteins that comprise the LINC complex in various colors (Suns, Nesprins, Filament proteins).



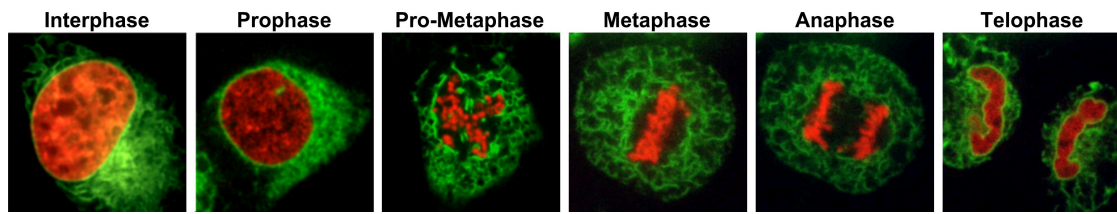
**Chapter I Figure 2: TEM of HeLa cell indicating nuclear and cytoplasmic spaces.**

TEM cryo-fixed image panels of a single HeLa cervical cancer cell. HeLa cells were grown on sapphire disks and cryo-preserved, followed by sectioning and staining with uranyl acetate to enhance structure contrast. Visible cytoplasm with cellular organelles (mitochondria, liposomes, ER and golgi) appear in the left panel, middle panel shows the nuclear envelope outlined in black compared to cell body additionally outlined in the right panel to illustrate the scale of the nucleus within the cell.



**Chapter I Figure 3: Life cycle of the metazoan cell.**

Representative images of metazoan cells indicated interphase and the various phases of mitosis. U2OS cells expressing GFP-Sec61 $\beta$ -fragment and H2B-tdTomato imaged in real time using spinning disk confocal microscopy from interphase through mitosis with still frames from individual cells representing each phase. Chromatin condensation begins in prophase, the NE is torn apart and absorbed into the ER during the transition to metaphase (pro-metaphase). Upon completed NE breakdown, chromosomes are collected and aligned at the metaphase plate (metaphase). Chromatin masses are pulled to opposite poles of the cell to achieve complete chromosome segregation in anaphase. The NE is reformed beginning in late anaphase with complete nuclear rings visible by the end of telophase.



## CHAPTER II

Recruitment of functionally distinct membrane proteins to chromatin mediates nuclear envelope formation *in vivo*.

**Abstract**

Formation of the nuclear envelope (NE) around segregated chromosomes occurs by the reshaping of the endoplasmic reticulum (ER), a reservoir for disassembled nuclear membrane components during mitosis. In this study, we show that inner nuclear membrane proteins such as lamin B receptor (LBR), MAN1, Lap2 $\beta$ , and the trans-membrane nucleoporins Ndc1 and POM121 drive the spreading of ER membranes into the emerging NE via their capacity to bind chromatin in a collaborative manner. Despite their redundant functions, decreasing the levels of any of these transmembrane proteins by RNAi-mediated knockdown delayed NE formation, whereas increasing the levels of any of them had the opposite effect. Furthermore, acceleration of NE formation interferes with chromosome separation during mitosis, indicating that the time frame over which chromatin becomes membrane enclosed is physiologically relevant and regulated. These data suggest that functionally distinct classes of chromatin-interacting membrane proteins, which are present at nonsaturating levels, collaborate to rapidly reestablish the nuclear compartment at the end of mitosis.

## Introduction

The nuclear envelope (NE) is composed of two lipid bilayers, the inner nuclear membrane (INM) and the outer nuclear membrane, which are fused at sites of nuclear pore complex (NPC) insertion.<sup>46</sup> Although the NE is continuous with the ER,<sup>47</sup> the INM contains a unique set of integral membrane proteins that provide functional interactions with chromatin and the nuclear lamina.<sup>48</sup> In metazoan cells, the nucleus disassembles at the onset of mitosis, facilitating spindle access to chromosomes.<sup>49</sup> During NE breakdown, transmembrane proteins of the NE are redistributed into the ER, which remains intact during mitosis.<sup>48,50</sup> Consequently, the sheet-like NE must reemerge from ER membranes during nuclear assembly.<sup>19,20,50</sup> We have recently shown that this massive membrane-restructuring event is initiated by the recruitment of tubule ends to chromatin.<sup>19</sup> This initial step is followed by the coating of the chromosome mass by ER membranes and their subsequent reorganization into the NE.<sup>20</sup> Although these results suggest that chromatin acts as a structural mediator of NE formation, the principle mechanism that generates the nuclear membrane from the ER remains unclear.

There is no agreement on whether the mitotic ER is entirely tubular<sup>23</sup> or largely composed of sheets.<sup>24</sup> We recently demonstrated that the removal of reticulons and DP1, which are membrane bending proteins that mediate

tubule formation,<sup>51</sup> from the reforming NE is rate limiting for nuclear assembly. This suggests that the transition of the ER into the flat NE leaflets requires a reduction in localized membrane curvature.<sup>47,52</sup> Thus, a mechanism must exist that counteracts membrane bending<sup>51</sup> and drives the local membrane spreading and redistribution around chromatin. One class of proteins that could fulfill such a function is the transmembrane proteins of the INM that have been shown to bind chromatin early during NE formation and have also been implicated in the targeting of membranes to chromosomes.<sup>53-55</sup> Although it has been postulated that such proteins are important for NE formation, the relative contributions of these proteins to the process in vivo are not well understood.

## **Results**

### **Measuring NE formation in vivo**

To analyze NE assembly in living cells, we used a previously established quantitative assay that allows us to determine the potential role of membrane proteins in NE formation by timelapse microscopy (Fig. 1 A).<sup>20,55,56</sup> In brief, we monitor the time between the initiation of chromosome separation ( $t = 0$ ), visualized by a histone H2B–tdTomato reporter, and the onset of nuclear accumulation of GFP-NLS, which marks the completion of NE

formation.<sup>21,56,57</sup> Using this assay, we determined that in U2OS and HeLa cells, NE formation was completed within ~10 min (Fig. 1, B and C).<sup>21,56</sup>

### **Reduced levels of INM proteins limit the rate of NE formation**

To test the potential involvement of NE proteins in promoting membrane targeting to and reshaping on chromatin, we reduced the levels of the INM proteins lamin B receptor (LBR), Lap2 $\beta$ , and MAN1, which were chosen because of their known ability to bind chromatin,<sup>58-61</sup> in U2OS cells using RNAi-mediated gene silencing (Fig. S1 A). We found that reductions of each of these proteins significantly delayed NE formation when compared with control cells transfected with scrambled RNA oligos (Fig. 1, B and C). Knockdown of the INM protein Sun1, which does not bind chromatin,<sup>9</sup> or the nucleoporin Nup107, whose reduction has been shown to block pore assembly,<sup>62</sup> had no significant effect on the onset of GFP-NLS accumulation (Fig. 1, B and C). This suggests that only a subset of NE proteins is involved in NE formation. The finding that depletion of LBR, Lap2 $\beta$ , or MAN1 resulted in a delay, but not a complete block of NE formation, indicated that each of these proteins functionally contributes to the formation of a closed NE in a manner consistent with built-in redundancy.

## **Functionally distinct chromatin-interacting proteins mediate NE formation**

Several INM proteins have been shown to bind DNA through different chromatin-associated proteins. For example, LBR interacts with heterochromatin protein 1,<sup>63</sup> whereas Lap2 $\beta$  and MAN1 bind to the barrier of autointegration factor (BAF) via their Lap2/emerin/Man1 (LEM) domains.<sup>64</sup> Therefore, it was important to test whether these INM proteins interact with chromatin at non-overlapping sites during nuclear assembly. If this were the case, the knockdown of BAF, which has been shown to be involved in NE formation,<sup>65-67</sup> should also delay but not block nuclear assembly. Indeed, we found that with efficient BAF depletion, NE formation occurred, but at significantly reduced rates (Fig. 1, B and C). NE formation delay with reduced BAF levels was more extreme than that seen with either Lap2 $\beta$  or Man1, which is consistent with the idea that BAF may mediate interactions between several proteins.

A recent study showed that several NE proteins, including the transmembrane nucleoporins Ndc1 and POM121, can bind DNA in vitro.<sup>68</sup> This raised the interesting possibility that functionally distinct classes of proteins, such as NPC components, might participate in NE formation. To test this, we knocked down Pom121 and Ndc1 and found that NE formation was significantly delayed (Fig. 1, B and C).<sup>69</sup> Importantly, although reduction

of Ndc1 slightly reduced the rate of transport, which is consistent with its role in NPC assembly,<sup>70</sup> it did not inhibit nuclear GFP-NLS accumulation (Fig. 1 B), suggesting that the observed delay in NE formation was not the result of a defect in NPC assembly. This is consistent with the finding that when the nuclear pore number (and thus transport rate) is reduced by the reduction of Nup107, the onset of import and NE formation times were similar to control cells (Fig. 1, B and C). Thus, the NE formation time reported by our assay is independent of transport rate. Collectively, these findings suggest that different classes of integral nuclear membrane proteins, which have the capacity to bind chromatin as a common feature, collaborate during mitosis to promote NE formation.

### **Reduction of BAF, Lap2 $\beta$ , or Ndc1 delays final stages of NE formation**

NE formation proceeds through two distinct steps: the targeting of membranes to chromatin and reshaping of ER membranes into an NE sheet.<sup>19</sup> To test whether INM proteins participate in NE sheet formation, we used a recently developed method and measured the fluorescence intensity of Sec61-GFP, an NE/ER marker, at the forming NE (Fig. S1, C and D).<sup>19,20</sup> Reduction of Lap2 $\beta$  or BAF did not significantly delay the increase in Sec61-GFP intensity during early stages of NE formation, suggesting that the initial targeting of ER membranes was not affected. Surprisingly, knockdown

of either protein was able to reduce Sec61-GFP intensity during the last few minutes of NE formation, suggesting that the final spreading of membranes around chromatin and subsequent closure are affected by the reduction of each of these proteins (Fig. S1D). Consistent with this, high-resolution imaging revealed that the reduction of either Lap2 $\beta$ , BAF, or Ndc1 protein levels delayed the appearance of a nuclear rim, which is an unequivocal indicator of the formation of a flat NE (Fig. 1, D and E).<sup>20</sup> Together, these data confirm the findings from the import assay and suggest that Lap2 $\beta$ , BAF, and Ndc1 reductions decrease the efficiency of NE formation during the final stages of assembly and closure.

### **INM proteins are positive regulators of NE formation**

Because multiple NE proteins collaborate in nuclear membrane formation, yet knockdowns of single components result in a significant delay in nuclear assembly, it is suggested that the concentrations of chromatin-binding NE proteins are nonsaturating at endogenous levels and that an excess of binding sites exist on chromatin. One prediction from this hypothesis is that the rate of NE formation is a function of the levels of chromatin-binding membrane proteins, and therefore, increasing their concentrations should accelerate nuclear assembly. To test this, we expressed V5-tagged versions of Lap2 $\beta$ , LBR, Pom121, and Ndc1. All

constructs were found to properly localize to the nuclear rim (Fig. S2 A), and Western blotting showed that these proteins were expressed at up to ~8 times the endogenous levels (unpublished data). Strikingly, cells expressing additional Lap2 $\beta$ , LBR, BAF, Pom121, or Ndc1 accelerated nuclear formation (Fig. 2, A and B). In contrast, the overexpression of the outer nuclear membrane protein nesprin-3a did not increase the rate of nuclear assembly (Fig. 2, A and B).<sup>71</sup> The latter suggests that the observed acceleration in NE formation is a phenomenon unique to proteins containing chromatin interaction domains. Interestingly, we did not observe additional acceleration of NE formation when Lap2 $\beta$  and LBR were coexpressed, suggesting that multiple rate-determining steps may exist and that other events, such as the previously described displacement of reticulons,<sup>20</sup> likely contributes to the maximum rate of nuclear assembly.

To further test the possibility that mediators of NE formation work collaboratively, we decided to perform combinations of NE protein knockdowns. We reduced the levels of LAP2B and LBR either alone or in combination and found that NE formation was delayed twice as much in cells with double knockdown compared with cells in which the levels of only one of the proteins had been reduced (Fig. 2 C). This suggests that these proteins have nonoverlapping functions and that recruitment of each protein to chromatin contributes to the rate of NE formation.

One prediction from this is that the knockdown of one INM protein should be rescued by the overexpression of a different chromatin-binding INM component. In support of this idea, we found that the delay in NE formation associated with Lap2 $\beta$  knockdown is attenuated in cells in which either BAF or LBR levels were transiently increased (Fig. 2 D and Fig. S2 C). Therefore, the rate of NE formation is at least in part determined by the relative amounts of INM proteins that can bind chromatin or DNA, and these proteins act in a highly redundant manner during assembly.

### **Nuclear targeting of Lap2 $\beta$ is independent of expression level**

To directly test whether the targeting of NE proteins to chromatin is not saturating at endogenous levels, U2OS cells were transfected with GFP-Lap2 $\beta$ , and the efficiency of NE targeting during nuclear assembly was measured 20 min after chromosome separation (Fig. 2 D). Consistent with the idea that there is an excess of binding sites for INM proteins on chromatin, the NE/ER ratio of GFP-Lap2 $\beta$  was constant over a wide range of expression levels. Therefore, we conclude that proteins involved in the targeting of membranes to chromatin promote NE formation and that at endogenous levels they limit the rate of assembly. The finding that each of these proteins limits the rate of nuclear assembly along with their nonsaturating concentrations implies an abundance of chromatin-docking sites. This notion

is consistent with recent findings that the bulk of NE proteins are completely cleared from the surrounding ER during the early stages of NE formation.<sup>19</sup>

### **Tethering of membranes to chromatin is required for NE formation acceleration**

To further characterize the molecular mechanisms by which INM proteins bind chromatin, we generated truncations of Lap2 $\beta$ , including the DNA and BAF-binding (LEM) domains as well as the lamin-interacting domain and transmembrane region (LMN + TM; Fig. 3 A). When a Lap2 $\beta$  fragment (LMN + TM) lacking both the DNA-binding and LEM domains was expressed, no significant change in the rate of NE formation was detected (Fig. 3, B and C) despite its localization to the NE (Fig. S2 B). This suggests that tethering of the transmembrane domain to the chromatin-interacting domains is required for promoting nuclear membrane formation. In contrast, when we overexpressed the DNA and LEM domains of Lap2 $\beta$  (Fig. 3 A), NE formation was significantly delayed, suggesting that these soluble fragments act as competitive inhibitors for the targeting of endogenous Lap2 $\beta$  or other LEM domain proteins to chromatin (Fig. 3, B and C). To directly test this, the DNA + LEM fragment was transfected into U2OS cells and endogenous Lap2 $\beta$  localization visualized by immunofluorescence (Fig. 3 D). In cells expressing the chromatin interaction fragment, endogenous Lap2 $\beta$  was found to be

greatly reduced at the NE in early G1 cells and was mainly found in perinuclear aggregates, suggesting a competitive inhibition by this fragment. Interestingly, in cells where endogenous Lap2 $\beta$  was displaced, as indicated by characteristic irregular NE staining, LBR targeting was unaffected (Fig. 3 E). This suggests that Lap2 $\beta$  and LBR promote NE assembly by tethering of the transmembrane domain to distinct chromatin sites, which is consistent with previous findings of nonoverlapping binding of LBR and Lap2 $\beta$  on chromatin.<sup>67</sup>

### **Accelerating NE formation decreases chromosome separation during mitosis**

The existence of multiple proteins that modulate the rate of NE formation as well as the finding that the process can be accelerated suggests that nuclear assembly is a highly regulated process. This raises the interesting question of whether imbalances in the levels of NE-forming proteins might interfere with normal cell cycle progression. To test this possibility, nuclear assembly was accelerated in U2OS cells by overexpressing LBR, Lap2 $\beta$ , or Ndc1, and the distance between segregating chromosomes was measured during anaphase as a function of time. Increasing the levels of each of these proteins caused a modest but significant decrease in the separation of chromosome clusters (Fig. 4, A and

C). Notably, we did not observe anaphase bridges, and therefore, it is unlikely that this phenotype stems from defects in global chromatin organization. We have previously shown that siRNA knockdown of reticulons 1, 3, and 4 in combination increases the rate on NE formation.<sup>20</sup> These ER proteins are excluded from chromosomes at all times and are therefore unlikely to affect chromatin organization. Additionally, the reduction of reticulons accelerated NE formation ~1.5 min faster than that demonstrated with the increased expression of NE proteins.<sup>20</sup> In cells with reduced reticulons, a striking impairment in the separation of chromosomes was observed (Fig. 4 B), suggesting that decreased chromosome separation was indeed caused by the premature spreading of membranes around the chromosome clusters, possibly inhibiting the ability for the mitotic spindle to pull the chromosome masses apart. This suggests that regulating the rate of NE formation may be necessary for proper cell cycle progression and thus is coordinated with other mitotic events in anaphase/telophase.

## **Conclusions**

In summary, our data suggest that endogenous concentrations of NE-promoting transmembrane proteins limit the rate of nuclear assembly as indicated by their overexpression accelerating the process (Fig. 2, A and B). NE formation is also affected by endogenous levels of the ER-shaping

reticulum proteins that slow NE formation. These findings suggest a tug of war between reticulons and their membrane-curving activity and NE proteins, which promote membrane attachment and spreading around chromatin.<sup>20</sup> We propose that the massive membrane-restructuring event that results in the formation of the sheet-like NE involves functionally diverse groups of NE proteins that collaborate during mitosis to tether membranes to the chromatin surface and thereby drive NE formation.

Our findings suggest that NE formation relies on the intrinsic propensity of the ER to efficiently transition between tubules and sheets to reorganize membranes at the chromatin surface into the forming NE at the conclusion of each mitotic cycle.<sup>47</sup> To shift this equilibrium toward sheet formation, the chromatin-binding capacity of NE proteins is used to coat the entire chromosome mass with a closed NE. This massive membrane-restructuring event is accomplished by the collaboration of functionally distinct classes of NE proteins and their ability to bind chromatin. Our findings are consistent with the idea that INM proteins serve to anchor ER membranes at the chromatin surface and promote the morphological changes associated with the spreading of the membranes onto and around the chromatin surface (Fig. 4 D).<sup>19</sup> It remains to be seen whether chromatin-mediated tubule to sheet transitions or the recruitment of ER sheets is the main mechanism of NE formation, although both ideas are not mutually exclusive.

In principle, the number of NE-forming transmembrane proteins might be substantial, as ~40 NE proteins exhibit DNA binding potential.<sup>68</sup> Notably, although proteins like Lap2 $\beta$  and LBR appear to interact with chromatin in a nonoverlapping fashion, reductions in either one or both of these proteins is unable to completely block NE formation and is indicative of a redundant system. The large number of NE proteins may provide a fail-safe mechanism, increasing the reliability of NE formation by multiplying critical components. In such a system, if a single NE-promoting protein fails to target, NE formation can still be accomplished, although possibly at a slower rate. This is consistent with the finding that despite the observed collaboration, many of these proteins contribute to the overall rate of NE formation. In light of the finding that acceleration of NE formation interferes with normal chromosome separation during mitosis, the proposed regulatory role of NE membrane proteins may be relevant to human disease. It will be interesting to test whether such a defect occurs in cancer cells in which the up-regulation of Lap2 $\beta$  has recently been described.<sup>72</sup>

## **Materials and Methods**

### **Molecular constructs and antibodies**

Human Lap2 $\beta$ , LBR, BAF, Ndc1, Pom121, and nesprin-3a were amplified by PCR from IMAGE clones (Open Biosystems) and inserted into

the V5- containing pcDNA6.2/Lumio (V5 of either N or C terminus) vectors using Gateway cloning (Invitrogen). Fragments of human Lap2 $\beta$  were amplified by PCR and inserted into pcDNA6.2/Lumio using Gateway cloning. Full- length Lap2 $\beta$  was also inserted into the N-terminal GFP-containing vector pCDNA6.2/Dest53 using Gateway cloning. Sec61-GFP and H2B-tdTomato were previously described; in brief, a fragment of Sec61 (aa 1–65) was amplified by PCR and cloned as a C-terminal fusion to GFP, and the H2B construct was provided by G. Pearson (The Salk Institute for Biological Studies, La Jolla, CA) and is a C-terminal fusion to tdTomato.<sup>20</sup> Antibodies against V5 (mouse [Invitrogen] and rabbit [Novus Biologicals]), BAF (Novus Biologicals), Sun1 (Abcam), tubulin (Sigma-Aldrich), LBR (Abcam), and calreticulin (Novus Biologicals) are commercially available. Antibodies against Lap2 $\beta$  were provided by the laboratory of R. Foisner (Medical University of Vienna, Vienna, Austria). Antibodies against Ndc1 were provided by the laboratory of U. Kutay (ETH Zürich, Zürich, Switzerland).<sup>69</sup> Antibodies for Pom121 were generated in a rabbit host against aa 448–647 of murine Pom121 fused to GST. Monoclonal antibodies against the V5 epitope were used at a dilution of 1:1,000 for indirect immunofluorescence and 1:5,000 for Western blotting. Monoclonal antibodies against Lap2 $\beta$  were used 1:1 for both indirect immunofluorescence and Western blotting. Antibodies against BAF were used at a dilution 1:500, antibodies against LBR were used at a dilution of 1:1,000, antibodies against Sun1 were used at a dilution of 1:500,

unpurified serum against Pom121 was used at a dilution of 1:500, antibodies against Nup107 were used at a dilution of 1:500, and antibodies against Ndc1 were used at a dilution of 1:500 for Western blotting.

### **Cell transfection and live cell imaging**

U2OS cells were grown and imaged in DME with 10% fetal bovine serum with 1× antibiotic antimycotic (Invitrogen). Cells were plated on 8-well micro-slides (iBidi) and transfected with 0.6 µl Lipfectamine2000 (Invitrogen) and 0.3 µg of each DNA construct 2 d before live cell imaging as recommended by Invitrogen. For siRNA knockdown, cells were transfected with 25 nmol RNA 2 and 4 d before imaging. siRNA oligo sequences used were as follows:

Lap2β, 5'-AGG CAU UAA CUA GGG AAU dTdT-3';

LBR, LBR Stealth Select RNAi HSS105976;

BAF, 5'-GGC CUA UGU UGU CCU UGG CdTdT-3';

Ndc1, 5'-CUG CAC CAC AGU AUU UAU A-3';

Rtn1, 5'-UAG AUG CGG AAA CUG AUG GTT-3';

Rtn3, 5'-CCU UCU AAU UCU UGC UGA ATT-3';

Rtn4, 5'-GAA UCU GAA GUU GCU AUA TT-3';

Nup107, 5'-CUG CGA AUA CAC UUU CCU CTT-3';

Sun1, 5'-CCA UCC UGU AUA CCU GUC UGU AU-3';

Pom121, 5'-CAG UGG CAG UGG ACA UUC A-3';

scrambled, 5'-UAG AUA CCA UGC ACA AUC CTT-3' (Invitrogen).

Live cells were imaged at 37°C maintained by air stream incubator and enriched with CO<sub>2</sub> (Solent Scientific). Time-lapse images were taken on a spinning-disk confocal microscope (Yokogawa) built around an inverted stage microscope (DMRIE2; Leica). Images were captured on an EM charge-coupled device digital camera (Hamamatsu Photonics) and acquired using SimplePCI (Compix). Cells were imaged using a 63× oil emersion objective with a 1.4 numerical aperture (Leica). Fluorochromes used in this study are EGFP, tdTomato, Alexa Fluor 488, and Alexa Fluor 568.

### **Image analysis and statistics**

Images were analyzed using Photoshop (version CS4; Adobe) extended, and statistics used were as described previously; in brief, mean pixel intensity was measured by selecting regions of interest, resulting data were analyzed in Excel (Microsoft), and distances were measured in micrometers by selection.<sup>20</sup>

### **Online supplemental material**

Fig. S1 shows confirmation of siRNA knockdown efficiencies, membrane recruitment to chromatin under knockdown conditions for various proteins, and NE/ER ratio for Lap2B-GFP at varying expression levels. Fig. S2 shows localization of epitope-tagged constructs by immunofluorescence. Tables S1–S3 show statistics for the average NE formation time for the

treatments used in this study. Online supplemental material is available at <http://www.jcb.org/cgi/content/full/jcb.200901106/DC1>.

## **ACKNOWLEDGEMENTS.**

Chapter 2, in full, consists of the following publication:

Anderson DJ\*, Vargas JD\*, Hsiao JP, Hetzer MW. 2009. Recruitment of functionally distinct membrane proteins to chromatin mediates nuclear envelope formation in vivo. *JCB* 186(2):183-91

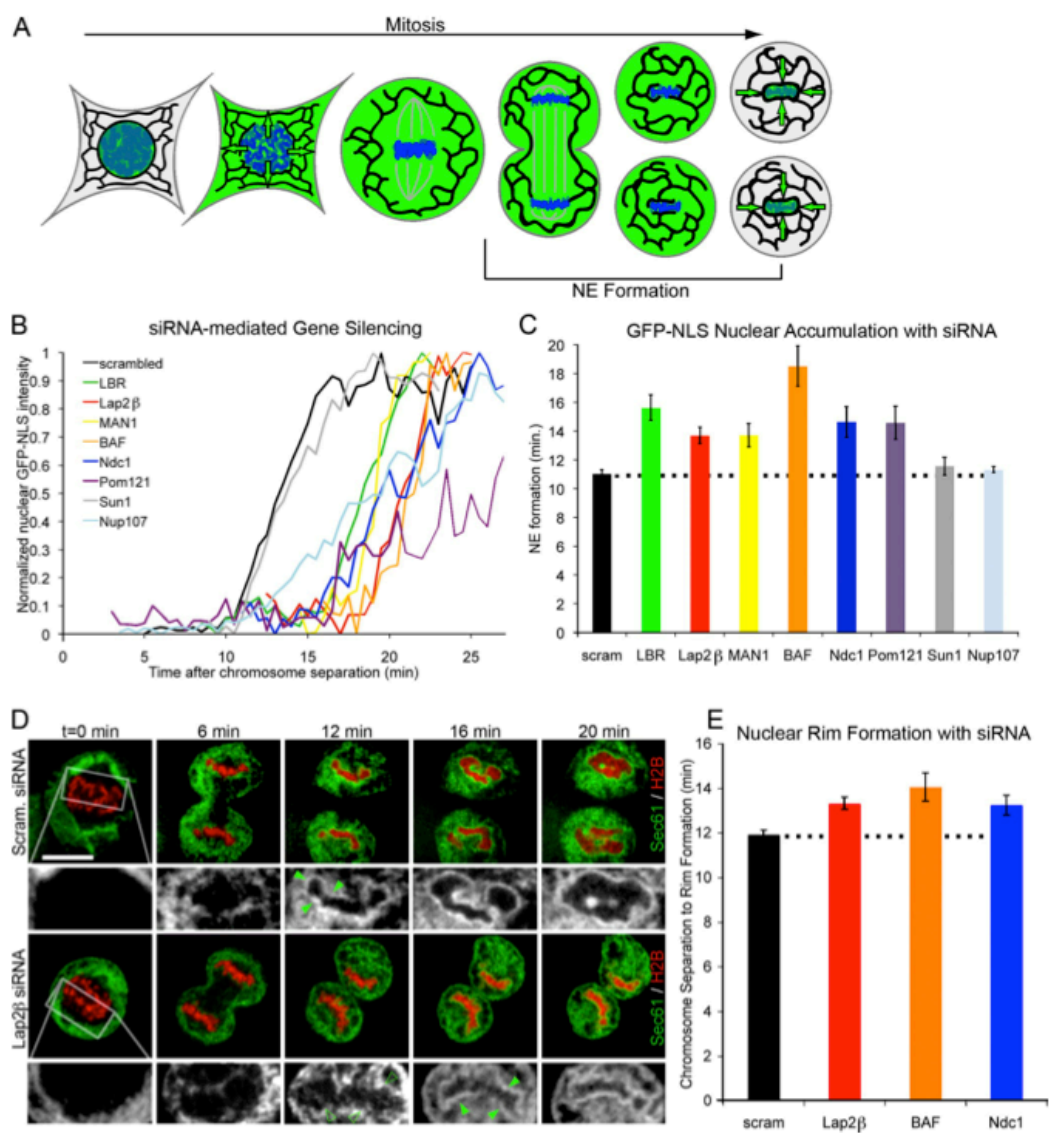
(\*co-first authors)

©Anderson et al., 2009. **JCB**. doi: 10.1083/jcb.200901106

Daniel Anderson and I were the primary researchers and authors for these studies under the supervision and direction of Martin Hetzer. Joshua Hsia contributed to the cloning of constructs used in this study. I would like to thank Maximiliano D'Angelo, Maya Capelson, Christine Doucet, Walter Eckhart, Sebastian Gomez, Tony Hunter, Yun Liang, Robbie Schulte, Jessica Talamas, Matthew Weitzman, and Susan Wentz for critically reading the manuscript of this work. This work was supported by the National Institute of General Medical Sciences (award number R01GM073994).

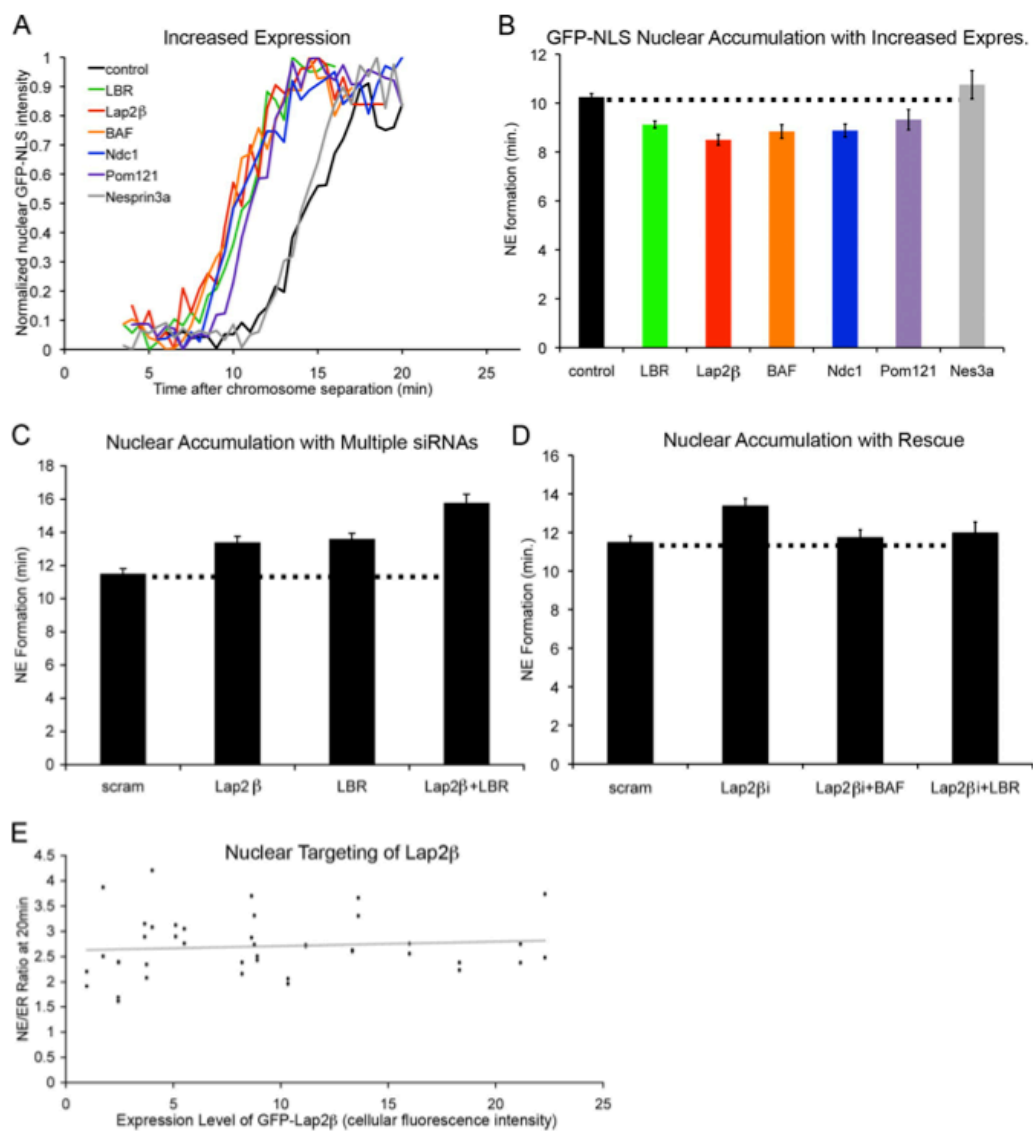
**Chapter II Figure 1: Chromatin-binding NE proteins collaborate during NE formation.**

(A) Diagram shows the dynamic localization of nuclear-targeted GFP (green) during open mitosis. Reaccumulation of GFP-NLS into daughter nuclei serves as an indicator for completed NE formation. (B) Cells were transfected with H2B-tdTomato and GFP-NLS and imaged through mitosis. Representative traces of chromatin-localized GFP-NLS in which  $t = 0$  is set at the onset of chromosome separation show the time required for NE formation in U2OS cells with reduction of protein levels by siRNA knockdown. (C) Average time from chromosome separation to GFP-NLS nuclear accumulation was plotted.  $n > 20$  for each condition (Table S1) with  $P < 0.01$  when LBR, Lap2 $\beta$ , MAN1, BAF, Ndc1, or Pom121 siRNA was compared with scrambled (scram) RNA control, and  $P = 0.23$  and  $0.20$  for Sun1 and Nup107, respectively (by  $t$  test). (D) U2OS cells were transfected with H2B-tdTomato (red) and Sec61-GFP (green, black, and white insets) and imaged from mitosis. Nuclear rim formation was compared in cells transfected with scrambled RNA or siRNA against Lap2 $\beta$  (closed arrowheads). After 12 min, no nuclear rim was detected with the knockdown of Lap2 $\beta$  (open arrowheads) compared with rim signal present in scrambled siRNA controls. Outlined areas represent the regions that are magnified below. Bar, 20  $\mu\text{m}$ . (E) Average time from chromosome separation to complete nuclear rim formation was plotted.  $P < 0.01$  when Lap2 $\beta$ , BAF, or Ndc1 knockdown was compared with scrambled RNA. Dotted lines indicate control cell timing. Error bars indicate SEM.



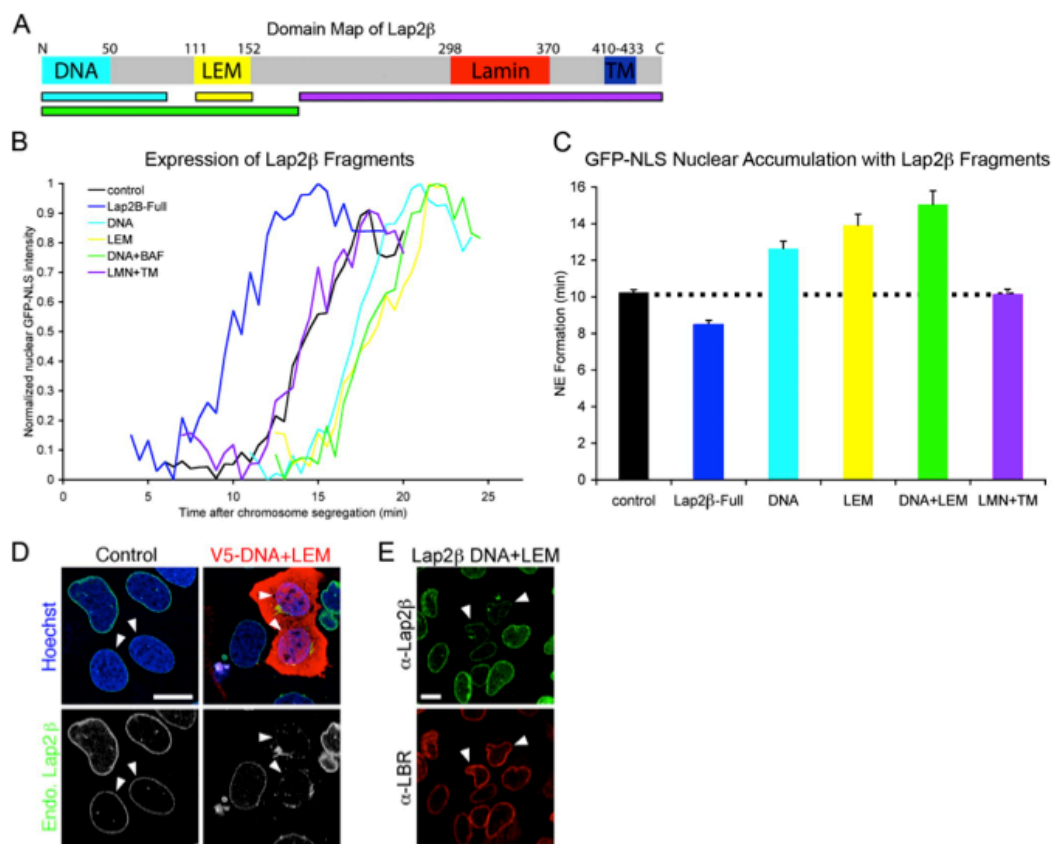
**Chapter II Figure 2: Chromatin-interacting NE proteins promote nuclear assembly.**

(A) Cells were transfected as in Fig. 1 B and imaged through mitosis. Representative traces of chromatin-localized GFP-NLS in which  $t = 0$  is set at the onset of chromosome separation show the time required for NE formation in U2OS cells in which protein levels were increased by transfection with epitope-tagged constructs. (B) Average time from chromosome separation to GFP-NLS nuclear accumulation was plotted.  $P < 0.001$  when Lap2 $\beta$ , LBR, BAF, Ndc1, or Pom121 increased expression (expres) was compared with control cells, and  $P = 0.20$  for nesprin-3a (Nes3a; Table S2). (C) NE formation time was measured after partial knockdown of Lap2 $\beta$ , LBR, or both with a single round of siRNA transfection when Lap2 $\beta$  or LBR were compared with scrambled (scram) RNA oligos or when Lap2 $\beta$  + LBR was compared with Lap2 $\beta$  or LBR alone ( $P < 0.001$ ; Table S3). (D) NE formation time was measured after partial knockdown of Lap2 $\beta$  combined with overexpression of either BAF or LBR and compared with the partial knockdown alone ( $P > 0.20$  for each). (E) U2OS cells were transfected with GFP-Lap2 $\beta$  and H2B-tdTomato and imaged through mitosis. Average GFP fluorescence intensity was measured over entire cell and plotted against the ratio of GFP-Lap2 $\beta$  at the NE to peripheral GFP-Lap2 $\beta$  (NE/ER ratio).  $n > 20$  for each condition (Table S3). Dotted lines indicate control cell timing. Error bars indicate SEM.



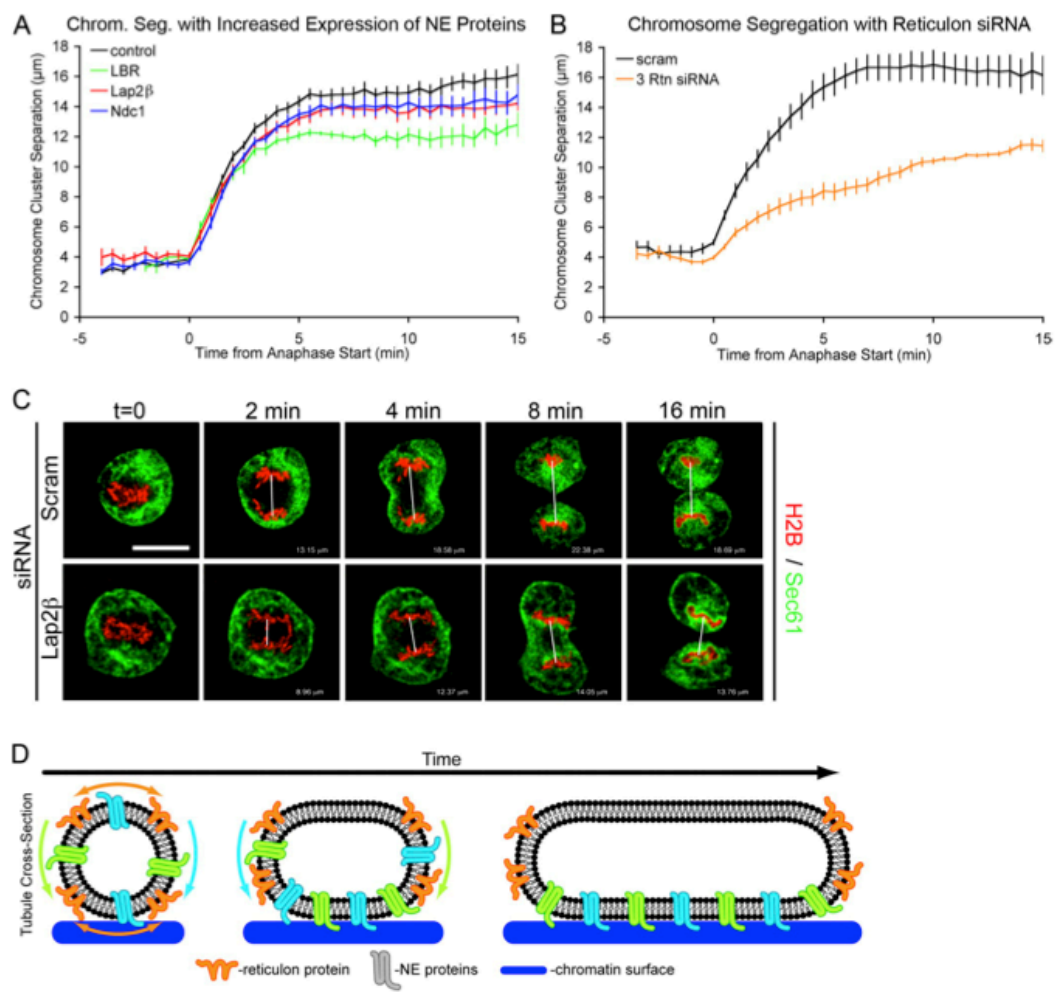
**Chapter II Figure 3: Membrane–chromatin tethering function of Lap2 $\beta$  in NE formation.**

(A) Map of Lap2 $\beta$  shows distinct functional domains that interact with DNA, BAF (LEM), lamins, and lipid bilayer (TM). (B) Representative traces of chromatin-localized GFP-NLS in which  $t = 0$  is set at the onset of chromosome separation show the time required for NE formation in U2OS cells where fragments of Lap2 $\beta$ , DNA, LEM, DNA + LEM, or LMN + lipid bilayer have been overexpressed. (C) NE formation time was measured with the expression of Lap2 $\beta$  fragments.  $n > 40$  for each fragment.  $P < 0.001$  for the expression of DNA, LEM, and DNA + LEM fragments when compared with control cells;  $P = 0.4$  for LMN + TM. Dotted line indicates control cell timing. Error bars indicate SEM. (D) U2OS cells were transfected with the V5-DNA + LEM fragment of Lap2 $\beta$  and stained with antibodies against V5 (red) and endogenous (endo) Lap2 $\beta$  (green). Arrowheads indicate early G1 cells as indicated by nuclear size and paired orientation. (E) U2OS cells were transfected with the DNA + LEM fragment of Lap2 $\beta$  and stained with antibodies against endogenous Lap2 $\beta$  and LBR. Arrowheads indicate cells where endogenous Lap2 $\beta$ , but not LBR, is displaced by the chromatin-binding domain of Lap2 $\beta$ . Bars, 20  $\mu\text{m}$ .



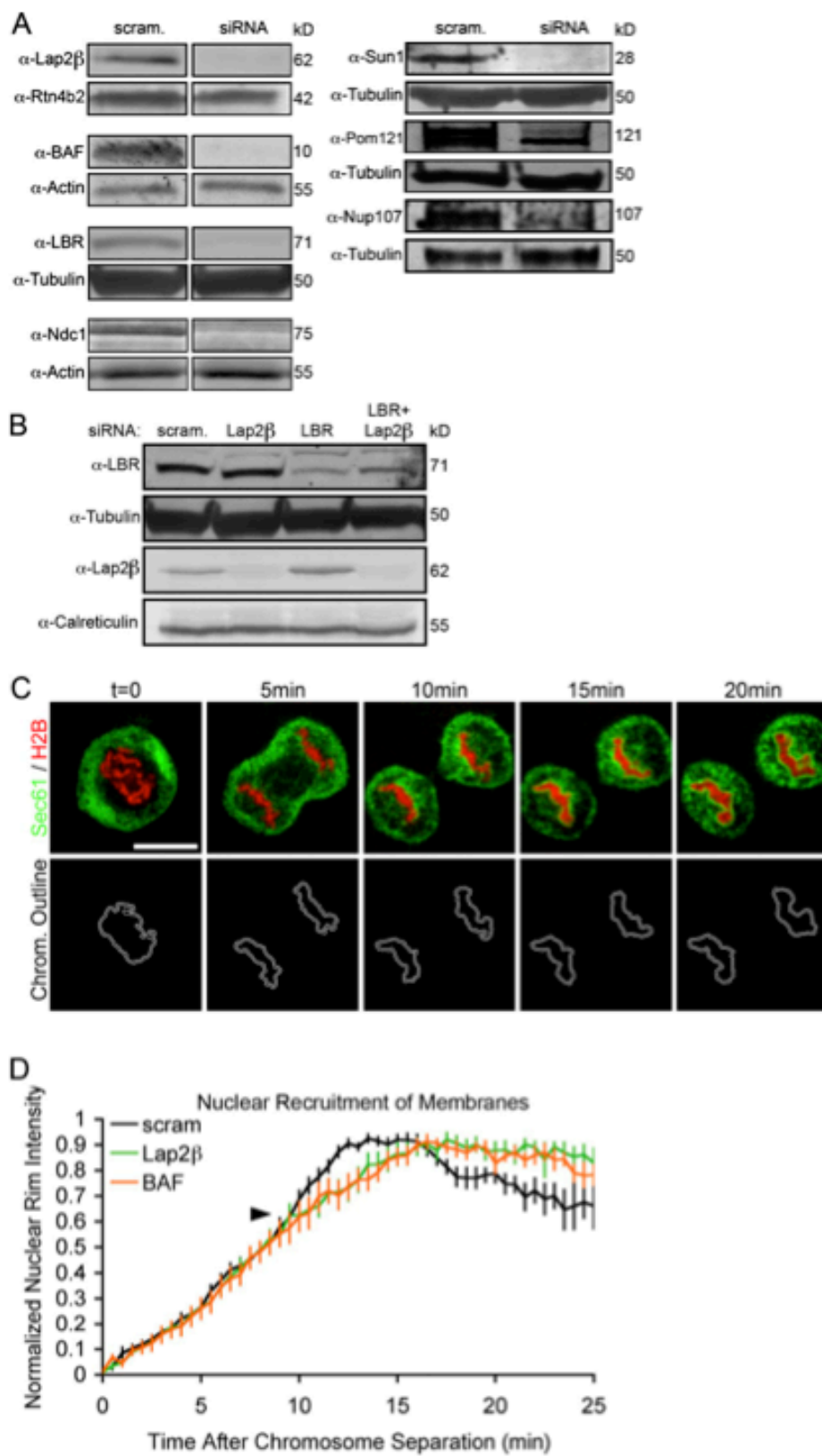
**Chapter II Figure 4: Acceleration of nuclear membrane formation causes chromosome segregation defect.**

(A) Mitosis was analyzed by transfecting U2OS cells with Sec61-GFP and H2B-tdTomato and comparing control cells with cells in which NE formation was accelerated by overexpression of LBR, Lap2 $\beta$ , or Ndc1. Chromosome cluster separation (chrom seg) is plotted over time with  $P < 0.001$  for Boltzmann Sigmoidal curve fitting to control cells. (B) Chromosome cluster separation plotted over time for extreme NE formation acceleration caused by the siRNA knockdown of reticulons 1, 3, and 4. (C) Representative images of U2OS cells with Sec61-GFP (green) and H2B-tdTomato (red) compares control cells with cells in which NE formation was accelerated by overexpression of Lap2 $\beta$ , and the distance between chromosome clusters was measured.  $t = 0$  is set at anaphase onset. White lines indicate distances measured in Photo-shop extended. Bar, 20  $\mu\text{m}$ . (D) Cross-sectional schematic of a membrane tubule expanding onto chromatin (blue). Reticulons (orange) are displaced from the flat membrane where INM proteins (green) are targeted to chromatin and drive membrane expansion around chromatin. Error bars indicate SEM.



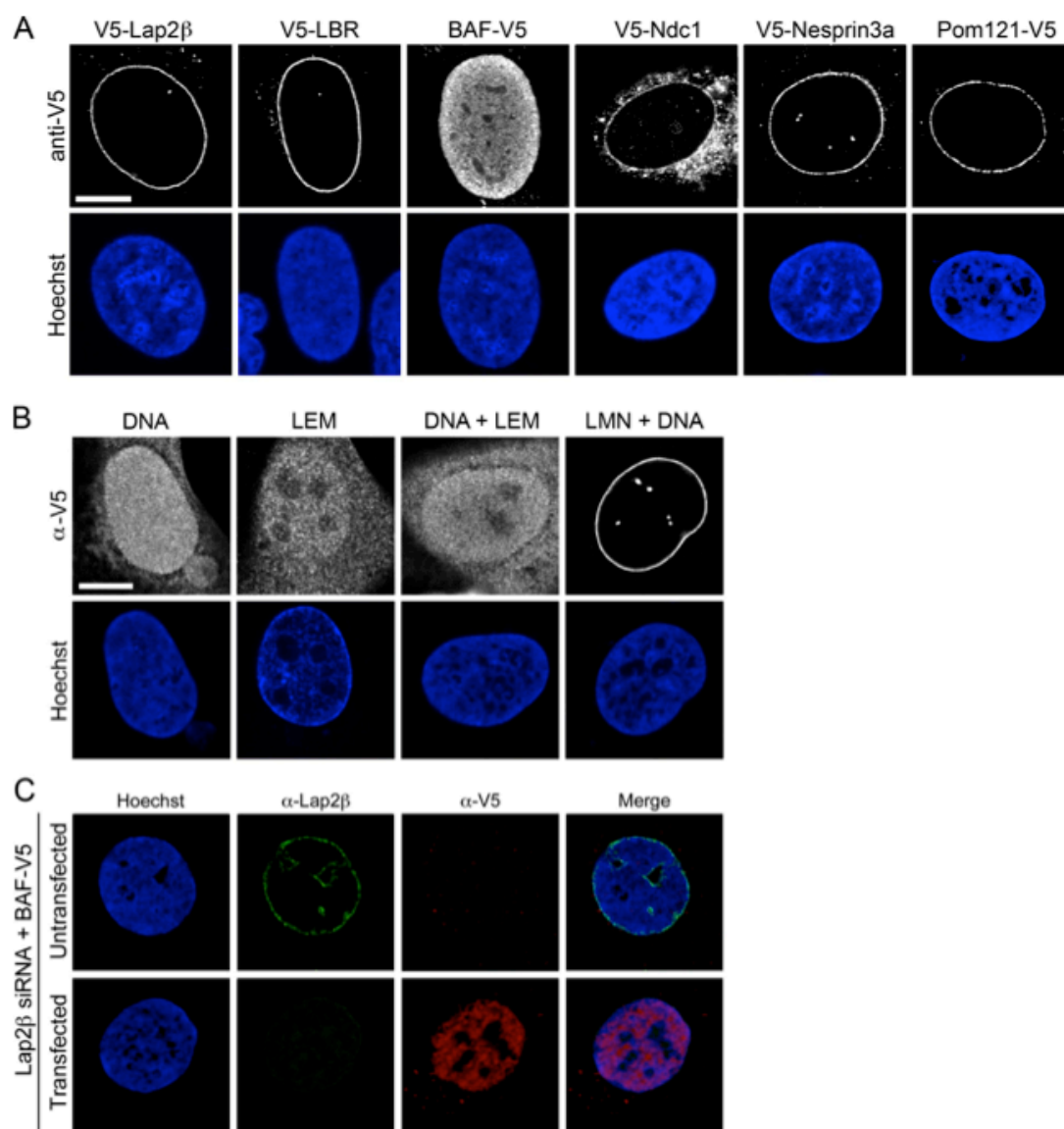
**Chapter II Supplemental Figure 1: Reduction of chromatin-binding proteins delays accumulation of membranes at the chromatin surface during NE formation.**

(A) Reduction of protein levels by siRNA-mediated gene silencing was measured by Western blot analysis using antibodies that detect endogenous Lap2 $\beta$ , BAF, LBR, Ndc1, Sun1, Pom121, or Nup107. (B) Reduction of either Lap2 $\beta$  or LBR by siRNA-mediated knockdown followed by Western blot analysis with antibodies against both Lap2 $\beta$  and LBR shows levels of both proteins obtained under each knockdown condition. (C) Intensity of Sec61-GFP at the forming NE was quantified for reductions in either Lap2 $\beta$  or BAF and compared with scrambled siRNA control by measuring fluorescence signal in a border directly around chromatin over time, with  $t = 0$  set at the metaphase to anaphase transition. Bar, 20  $\mu\text{m}$ . (D) Sec61-GFP intensity at the forming NE was measured in cells in which Lap2 $\beta$  (green) or BAF (orange) protein levels were reduced by siRNA and compared with cells transfected with scrambled (scram) siRNA (black). Arrowhead indicates where curves begin to deviate. Error bars indicate SEM.



**Chapter II Supplemental Figure 2: Localization of V5-tagged constructs.**

(A) Localization of V5-tagged Lap2 $\beta$ , LBR, BAF, Ndc1, and nesprin-3a was characterized by immunofluorescence. (B) Localization of V5-tagged fragments of Lap2 $\beta$  was characterized by immunofluorescence. (C) Efficiency of simultaneous knockdown and overexpression is shown for U2OS cells reduced with Lap2 $\beta$  siRNA and transiently transfected with BAF-V5 (bottom) compared with untransfected cells (top) on the same coverslip to ensure similar antibody staining and imaging parameters. Bars, 20  $\mu$ m.



**Chapter II Table S1: Average NEF times and statistics for siRNA-mediated knockdown of selected proteins.**

siRNAs	NEF time (min)	SEM	P-value	n
Scrambled	11.0500	0.2674	NA	80
Lap2 $\beta$	13.7045	0.5695	9.94983E-05	22
LBR	15.6500	0.8930	2.90203E-05	20
MAN1	13.7368	0.8206	0.001606941	38
BAF	18.5208	1.3875	3.58773E-05	16
Ndc1	14.6429	1.0618	0.001295758	28
Pom121	14.6000	1.1633	0.003090964	25
Sun1	11.5714	0.6221	0.225576544	14
Nup107	11.3380	0.2067	0.197749598	71

NEF, NE formation; NA, not applicable. P-values are calculated by t test compared with scrambled siRNA control.

**Chapter II Table S2: Average NEF times and statistics for transiently increased expression levels of selected proteins.**

<b>Overexpression constructs</b>	<b>NEF time</b>	<b>SEM</b>	<b>P-value</b>	<b>n</b>
	(min)			
Control	10.2437	0.1563	NA	145
Lap2 $\beta$	8.5000	0.2149	1.13863E-09	42
LBR	9.1250	0.1449	8.75001E-08	68
BAF	8.8409	0.2780	4.21248E-05	22
Ndc1	8.8788	0.2656	1.85933E-05	33
Pom121	9.3269	0.4132	0.000371853	26
Nes3a	10.7500	0.5775	0.202391077	20

NEF, NE formation; NA, not applicable. P-values are calculated by t test compared with reporter-only transfection control.

**Chapter II Table S3: Average NEF times and statistics for combination siRNA and kinetic rescue experiments.**

Experimental treatments	NEF time (min)	SEM	P-value	n
Scrambled	11.5000	0.3145	NA	31
Lap2 $\beta$ siRNA	13.3963	0.3695	8.48754E-05	82
LBR siRNA	13.6032	0.3436	1.00555E-05	63
Lap2 $\beta$ + LBR siRNAs	15.7841	0.5009	0.0002 <sup>a</sup>	44
Lap2 $\beta$ siRNA + BAF-V5	11.7581	0.3809	0.301685638	31
Lap2 $\beta$ siRNA + LBR-V5	12.0000	0.5434	0.215404785	24

NEF, NE formation; NA, not applicable. P-values are calculated by t test compared with scrambled siRNA control. <sup>a</sup>P = 0.0002 compared with LBR; P = 0.0001 compare with Lap2 $\beta$ .

## CHAPTER III

Transient nuclear envelope rupturing during interphase in human cancer cells

**Abstract**

Neoplastic cells are often characterized by specific morphological abnormalities of the nuclear envelope (NE), which have been used for cancer diagnosis for more than a century. The NE is a double phospholipid bilayer that encapsulates the nuclear genome, regulates all nuclear trafficking of RNAs and proteins and prevents the passive diffusion of macromolecules between the nucleoplasm and the cytoplasm. Whether there is a consequence to the proper functioning of the cell and loss of structural integrity of the nucleus remains unclear. Using live cell imaging, we characterize a phenomenon wherein nuclei of several proliferating human cancer cell lines become temporarily ruptured during interphase. Strikingly, NE rupturing was associated with the mislocalization of nucleoplasmic and cytoplasmic proteins and, in the most extreme cases, the entrapment of cytoplasmic organelles in the nuclear interior. In addition, we observed the formation of micronuclei-like structures during interphase and the movement of chromatin out of the nuclear space. The frequency of these NE rupturing events was higher in cells in which the nuclear lamina, a network of intermediate filaments providing mechanical support to the NE, was not properly formed. Our data uncover the existence of a NE instability that has the potential to change the genomic landscape of cancer cells.

## Introduction

The nuclear envelope (NE) is a physical membrane barrier that separates the nucleus from the cytoplasm. It fulfills at least two essential functions in eukaryotic cells: first it regulates the movement of molecules between the nucleus and the cytoplasm by active, signal-dependent transport via aqueous channels that are formed by the nuclear pore complexes (NPCs), and second it creates a permeability barrier that prevents the passive diffusion of molecules larger than ~40 kDa across the NE. An intact nuclear permeability barrier is generally considered to be a prerequisite for nuclear transport and to be critical for proper cell compartmentalization.

Morphologically and structurally abnormal nuclei are frequently observed in cancer cells.<sup>73</sup> Morphometric criteria such as NE invaginations, extrusions and lobes are routinely used in the clinic for cancer diagnostics and prognosis,<sup>74</sup> and in some cases, karyometric features were found to be more appropriate than biomarkers to predict metastases.<sup>35</sup> Despite the clinical relevance of aberrant NE morphology, it remains unclear why such changes to the NE are more prevalent in cancer cells, and if these characteristic morphological features of the NE contribute to cell transformation and tumor formation. The nuclear lamina is an intermediate filament network comprised of lamin proteins that assembles on the inner nuclear membrane (INM). It is connected to the NE via interactions with INM proteins and provides structural support,

mechanical stiffness and elasticity to the nuclear membrane. Two major types of lamin are present in human somatic cells: the A-type lamins include lamin A and lamin C, which are different isoforms of a single gene, and the B-type lamins that include lamin B1 and lamin B2, which are encoded by separate genes. Both types of lamins are important for stabilizing the nuclear membrane,<sup>75-78</sup> and, along with various interacting proteins, are thought to organize the nucleus by localizing specific proteins responsible for chromatin organization, cell cycle control, and transcription regulation to the nuclear periphery.<sup>79</sup> Lamin B1 is important for development; mice homozygous for non-functional lamin B1 die at birth.<sup>80</sup> In addition, mutations in the lamin genes that alter lamin protein expression and disrupt the formation of the lamina cause a group of pleiotropic developmental diseases called laminopathies.<sup>6</sup> These disorders are characterized by changes in the mechanical properties of the nucleus<sup>75,81-83</sup> and affect mainly cells under mechanical stress.<sup>84</sup>

The NE is a dynamic structure that undergoes complete disassembly and reformation during the cell cycle. Nuclear envelope breakdown (NEBD) occurs only at the onset of mitosis and facilitates the equal segregation of the genome and other cellular components into two daughter cells. NEBD is initiated by a series of phosphorylation events that trigger the breakdown of the NPCs and lamina and is followed by the retraction of the NE into the mitotic endoplasmic reticulum (ER).<sup>60,85,86</sup> NE reformation during late

anaphase/telophase is a rapid process that involves distinct groups of INM proteins with redundant functions driving a rapid and massive reorganization of the ER to surround the decondensing chromatin.<sup>20,21,87,88</sup>

Given the functional importance of an intact NE, it was generally assumed that mixing of the cytoplasmic and nuclear compartments occurs only during mitosis. However, a recent study reported a temporary loss of cell compartmentalization by NE rupturing during interphase in cells isolated from laminopathy patients.<sup>89</sup> Since changes in NE structure are an early diagnostic criteria of malignant cell growth<sup>2</sup> and many cancer cells have decreased expression of lamins or other structural nuclear proteins both in tumors and in culture, we wondered whether nuclear membrane integrity is compromised in cancer cells.<sup>36,44,45,90-96</sup> Additionally, we were curious what might be the physiological consequences if lapses in interphase nuclear integrity occurs in cancer. Here we demonstrate that transient NE rupturing during interphase (NERDI), an event that involves an interphase loss of the nuclear permeability barrier and mixing of normally separated nuclear and cytoplasmic components, occurs in several commonly used human cancer cell lines. Further, we show that such ruptures result in significant mislocalization of nuclear and cytoplasmic factors. Our results suggest that this phenomenon may stimulate several fundamental processes associated with tumorigenesis like misregulation of growth signaling pathways and increased genomic instability.

## Results

### Transient mislocalization of nuclear GFP<sub>3</sub>-NLS in cancer cells.

To study potential defects in NE integrity in cancer cells, we used GFP<sub>3</sub>-NLS (three copies of GFP fused to the nuclear localization signal of the SV40 large T antigen) as a live-cell nuclear integrity reporter. Nuclear accumulation of this ~80 kD reporter occurs during interphase and requires both active nuclear import and the presence of an intact NE.<sup>20,55,87</sup> Localization of this reporter to the cytoplasm is indicative of NEBD, which occurs during early prophase (Fig. S1A NE in green, open arrows and Fig. S1B, open arrows) as the NE is retracted into the mitotic ER, and its re-localization to the nucleus in late anaphase/early telophase corresponds to NE reformation (Fig. S1A NE in green, solid arrows and Fig. S1B, solid arrows) and the resumption of active nuclear transport (Fig. S1A and B).<sup>20,55,60,85,87</sup> To test whether non-mitotic NE rupturing can also be visualized using this reporter, we transfected a human U2OS osteosarcoma cell line expressing GFP<sub>3</sub>-NLS with a FLAG tagged version of the HIV-1 protein Vpr, which has been shown to rupture the NE during interphase leading to cell cycle arrest in G2.<sup>97</sup> In contrast to control cells, GFP<sub>3</sub>-NLS was mislocalized to the cytoplasm in cells expressing Vpr-FLAG (Fig. S1C, arrows). Consistent with a previous report, Vpr-induced NE rupturing was extensive with nuclear ruptures persisting for several hours without repair (Fig. S1D).<sup>26</sup>

Having established a reliable assay to monitor NE integrity throughout the cell cycle, we transfected and monitored the localization of GFP<sub>3</sub>-NLS in U2OS cells over a period of at least 36 h. Images were acquired with a 3 min time interval to ensure that NE integrity was observed with sufficient temporal resolution throughout the cell cycle. We observed that in a rare subset of U2OS cells (~8% of cells in a population) GFP<sub>3</sub>-NLS transiently appeared in the cytoplasm concomitant with a decrease in nuclear signal and in the absence of mitotic division (Fig. 1A, Movie S1). Remarkably, the temporary efflux of GFP<sub>3</sub>-NLS out of the nucleus was followed by the proper re-accumulation of the reporter into the nucleus and these events could be observed to occur several times within individual cells (Fig.1A, arrows). To determine the kinetics of interphase NE ruptures we measured the fluorescence intensity of the GFP<sub>3</sub>-NLS in the nucleoplasm and cytoplasm over the course of this event. The loss of nuclear integrity was extremely rapid with virtually complete equilibration of nuclear and cytoplasmic GFP intensity occurring within a single frame (~3min) (Movie S1). This was followed by a slower recovery period on a timescale similar to that of post-mitotic NE reformation.<sup>20,87</sup>

In order to examine the dynamics of individual spilling events we employed curve fitting algorithms to interphase NE rupture events imaged with high (30 sec) temporal resolution. To calculate the rate of recovery after NERDI events, we measured the nuclear and cytoplasmic intensity of GFP<sub>3</sub>-

NLS and fit these intensities to a segmented regression where the intact nuclei were fit to a plateau constant, spilling events were fit to a linear regression and recovery events were fit to a sigmoidal curve (mean  $R^2 = 0.97$ ) (Fig.1B). We hypothesize that recovery after NERDI fits well to a sigmoidal curve rather than an exponential curve because nuclear import likely begins before ruptures are fully closed. This analysis gave recovery half-times of ~6 min although some cells seemed to struggle to repair the NE taking up to 9 min to reach the same 50% fluorescence recovery point (Fig.1B).

It is important to note that the frequency of NE rupturing during interphase (NERDI) did not increase with laser excitation intensity, exposure time, or expression level of the GFP<sub>3</sub>-NLS reporter (data not shown). Thus, it is unlikely that interphase loss of NE integrity is a result of experimental design or imaging. In addition, the disruption of the NE barrier did not result in apoptosis, as indicated by the ability of the cells to re-accumulate their nuclear contents, persist in culture, and go on to complete cell division and cytokinesis (Fig.1A, right panels; Movies S2 and S3).

To determine whether NERDI is specific to U2OS cells, we expressed and observed the dynamics of a nuclear reporter in two additional cancer cell lines, the human HeLa (cervical carcinoma) and SJSA (osteosarcoma) cell lines. We observed transient mislocalization of the reporter to the cytoplasm during interphase in both of these cell lines (Fig.1C), indicating that NERDI is not specific to U2OS cells and affects cancer cell lines arising from divergent

tissues. Importantly as a control, in primary human fibroblast IMR90 cells we observed less than 1% of cells exhibiting interphase NE rupture (Fig.2A). Our results from the single primary cell line are limited but suggest that NERDI may be more common in malignant cells and could correlate with the well-described alterations in NE structure in cancer cells.

Analyzing still images of NERDI in U2OS cells revealed that nuclear ruptures initiate from localized deformations of the NE (Fig. 1D, large arrows; Movie S4). These NE herniations expand and eventually rupture, with the observed efflux of GFP<sub>3</sub>-NLS appearing initially in the cytoplasmic region proximal to the site of NE herniation before rapidly diffusing throughout the cell body (Fig. 1D, small arrows; Movie S4). This observation suggests that interphase losses in nuclear integrity originate from large structural changes in the NE.

### **Knockdown of lamins increases the frequency of NE rupturing during interphase.**

Since aberrations in the nuclear lamina have been shown to affect the mechanical properties of the NE,<sup>26,98</sup> and since the NE herniations observed prior to rupturing are reminiscent of structures seen in cells lacking either lamin B1 or lamins A and C,<sup>80,81</sup> we reasoned that altered lamin organization might be facilitating interphase nuclear rupturing in U2OS cells. To test this

idea, we treated U2OS cells with either a scrambled siRNA or a cocktail of siRNAs directed against the 3 nuclear lamin genes, lamin A/C, B1, and B2, that effectively targets each of the 3 lamins in individual cells (Fig. S2A). We found that transfection efficiency limited the population-averaged reduction in lamin protein levels to ~20% by protein gel blot (Fig. S2B), and that this reduction led to a statistically significant ( $p < 0.05$ ) increase in the frequency of nuclear rupture events compared with control siRNA (Fig. 2A). In contrast, cells knocked down for the NPC components Nup93 or Nup107, or the INM proteins LBR and Lap2 $\beta$  in combination, had no statistically significant increase in NERDI frequency ( $p = 0.21, 0.34, \text{ and } 0.45$  respectively) (Fig. 2A). These results further support our model that NERDI is not due to changes in the passive diffusion limit, but rather to large-scale disruptions of the nucleus. Nuclear pore defects as a contributing factor to NERDI are made further unlikely by the rapid and mass movement of GFP<sub>3</sub>-NLS into the cytoplasm, which suggests a large temporary tear in the NE rather than a continual pore-associated leakiness.

Additional evidence for lamins normally functioning to prevent NERDI came from results from transmission electron microscopy (TEM) performed on U2OS cells stably expressing an shRNA against lamin B1 that resulted in a similar frequency (~25%) of NERDI as the triple siRNA cocktail. In lamin B1 shRNA cells stained with tannic acid to enhance the nuclear lamina (Fig.2B, solid arrows) nuclear herniations similar to those seen in live- imaging just

prior to NE rupture are clearly visible (Fig.2B, enlargements). Of note, areas where the NE is distended have a marked absence of electron density (Fig.2B, open arrows), suggesting that these areas, which are prone to rupture, are deficient in lamin assembly. The interior of the NE herniations often exhibit a gradation in staining by TEM with darker nucleoplasm-like material near the nuclear interior blending with lighter cytoplasmic-like material in the distal area of the herniation (Fig.2B), as would be expected if the nuclear and cytoplasmic compartments had previously mixed at this location.

In addition to the increased NERDI frequency, the recovery time of cells treated with the triple lamin knock-down significantly increased ( $p < 0.05$ ) from an average of ~6 min for control cells to ~12 min for 3 lamin siRNA (Fig. 2C and D), indicating that lamins both prevent nuclear rupturing and promote the repair of NE rupturing. The ability of lamin reduction to increase the frequency of NERDI, as well as to increase the time required to recover from such defects further supports the idea that the observed phenomenon is a consequence of altered nuclear structure.

Our observations that NERDI increases with reduced lamin expression are particularly interesting since reduced and aberrant expression of nuclear lamins has previously been reported in tumor tissue.<sup>44,45,90-95</sup> Interestingly, we found that lamin levels were not uniform in U2OS cells; immunofluorescence using antibodies against lamin B1 and B2 revealed significant differences in

lamin staining within a single field of cells (Fig. S2C). This variation, which is also present in various cell cycle phases of U2OS cells synchronized by double thymidine block (data not shown), could underlie the differences in spilling frequency we observe in normal U2OS cells. Likewise, consistent with other reports,<sup>36,93,96</sup> we found that lamin protein levels also vary widely between different cancer cell lines as determined by protein gel blot (Fig. S2D). Of note, several breast cancer lines exhibited lower levels of lamin expression, including those classified as particularly invasive, compared with the non-transformed MCF-10A line that retains breast tissue specific differentiation characteristics (Fig. S2D). The lines with the most reduced lamin levels were not conducive to our live-imaging approach and so the presence of interphase nuclear rupturing in them remains uncertain.

Because depletion of lamins has been shown to have diverse effects on nuclear organization and functions,<sup>99,100</sup> we wanted to ensure the phenotype we observed was the result of changes in NE structure and not downstream effects on gene expression or chromatin reorganization. To do this, we overexpressed the other B-type lamin, lamin B2, in U2OS cells depleted of lamin B1 and observed NERDI frequency. Depletion of lamin B1 alone by shRNA gave a robust knock down of lamin B1 in individual cells (Fig. S3A) and an overall reduction in lamin B1 levels by protein gel blot (Fig. S3B). Lamin B2 functions similarly to lamin B1 in structuring the NE,<sup>99,101</sup> and our expression construct localized as expected in control U2OS cells and without

disrupting endogenous lamin B1 (Fig. S2E). While lamin B2 localizes to the NE similar to lamin B1, it is unlikely to have the same protein interactions, as lamin B2 null mice have distinct phenotypes.<sup>102</sup> We reasoned that expression of lamin B2 might compensate for the structural deficits of the lamin B1 depletion. To test this, U2OS cells stably depleted of lamin B1 were transfected with either mCherry-lamin B2 or mCherry alone. Expression of mCherry-lamin B2 was able to significantly decrease ( $p = 0.005$ ) the percentage of cells exhibiting NERDI, as well as decrease the average number of times each rupturing cell ruptured (Fig.2E), suggesting that it is the structural function of the lamins that normally maintains interphase nuclear integrity, and not their functions in interphase nuclear organization or transcription.

### **Interphase NE rupturing causes mislocalization of cellular components.**

Having established that our GFP-reporter is mislocalized to the cytoplasm during transient NE rupturing, we next wondered whether endogenous nucleoplasmic proteins would also be present in the cytoplasm during NE rupturing. Since our reporter for nuclear integrity is a soluble protein, we postulated that other soluble nuclear factors might be released into the cytoplasm during an interphase rupture event. We first characterized the localization of eIF4AIII, a member of the DEAD-box family of RNA

helicases and a soluble nuclear factor that is part of the exon junction complex loaded onto mRNAs inside the nucleus.<sup>103</sup> We observed eIF4AIII localizing in the nucleus and NE herniations during interphase by immunofluorescence in U2OS cells stably expressing an shRNA against lamin B1 (Fig.3A, top panels arrows). In cells with ruptured NEs, as identified by cytoplasmic GFP<sub>3</sub>-NLS localization and the absence of DNA condensation (Fig.3A, bottom panels arrows), eIF4AIII was mislocalized to the cytoplasm (Fig.3A), indicating that endogenous proteins are misplaced from the nucleus during NERDI. We also observed an increase in diffuse nuclear tubulin staining concomitant with NERDI (Fig.3A, middle panels solid vs. open arrows, see enlarged tubulin signal enhancement on right), suggesting that the loss of the permeability barrier across the NE occurs in both directions.

In order to confirm altered localization of cytoplasmic proteins during NERDI and that loss in nuclear integrity is bidirectional, we stained fixed U2OS cells expressing the lamin B1 shRNA with antibodies against UPF1, a cytoplasmic mRNA factor that is recruited upon recognition of a stop codon by the translation machinery.<sup>104</sup> Immunofluorescence imaging of U2OS cells stably reduced for lamin B1 to increase the frequency of NERDI showed that UPF1 is present within the interphase nucleus when nuclei undergo interphase rupture, as evidenced by GFP<sub>3</sub>-NLS presence in the cytoplasm (Fig.3B, top panels arrows). Again interphase rupture is distinguished from mitotic rupture by comparison to mitotic cells where the chromatin is clearly condensed and

the mitotic spindle is visible (Fig. 3B, bottom panels arrows). Although both cytoplasmic and nuclear proteins, specifically those involved in mRNA processing, are mislocalized during transient rupturing, it is plausible that their aberrant localization is corrected either by nuclear import/export machinery or during the next division cycle. In all observed cases their mislocalization coincided with a loss of nuclear integrity, as determined by efflux of GFP<sub>3</sub>-NLS from the nucleus. Therefore, it is likely that NERDI associated mislocalization of protein factors is recoverable as long as such factors carry appropriate localization signals, or in the worst case scenario factors could be reapportioned during the next mitotic cycle. Since peripheral chromatin is in close proximity to the NE via interactions with the lamina and INM proteins,<sup>105</sup> we wondered whether NERDI, which likely results in the disruption of these interactions, could result in the loss of genomic material from the nucleus. To test this possibility, we expressed H2B-mCherry, which localizes exclusively to chromatin throughout the cell cycle,<sup>87</sup> and GFP<sub>3</sub>-NLS in U2OS cells in which the three lamins had been depleted. Analysis of still images of an interphase NE rupture event clearly shows the presence of H2B-mCherry within NE deformations, as indicated by co-localization with GFP<sub>3</sub>-NLS (Fig.3C, left panels arrows). The presence of DNA in NE herniations is also supported by the observation of Hoechst labeling of these structures in immunofluorescent images of U2OS cells stably reduced for lamin B1 expression (see Fig. 3A). The NE deformation eventually ruptures, as

indicated by the diffuse cytoplasmic GFP<sub>3</sub>-NLS signal, and notably during this event H2B-mCherry also extends beyond the pre-rupture nuclear boundary, but with a more limited range (Fig. 3C, bottom panels arrows). The localization pattern of the H2B-mCherry signal is inconsistent with it being soluble and freely diffusible during the rupture (compare with GFP<sub>3</sub>-NLS, Fig.3C middle panels), and instead indicates that NERDI alters chromatin organization at the site of rupturing. After repair of the NE, indicated by nuclear accumulation of GFP<sub>3</sub>-NLS, H2B-mCherry remains segregated within an extra-nuclear body (Fig.3C, right panels arrows). Genomic instability is a hallmark of cancer and our data showing a persistent presence of chromatin outside the normal nuclear boundary make it plausible for premature rupturing of the NE to contribute to chromosome aberrations that accumulate over time in cancer cells. Our live-imaging results frequently show these extra-nuclear particles moving great distances from the post-rupture repaired NE (Movie S3). If these particles contain genomic information, the potential for mutagenesis is virtually certain.

### **NE rupturing causes temporary loss of cellular compartmentalization.**

We next asked whether mislocalization of cytosolic components during NERDI is limited to soluble proteins by examining organelle localization during NERDI. We examined mitochondria localization by expressing pTurboRFP-

mito in U2OS cells depleted of lamin B1 and expressing the integrity reporter GFP<sub>3</sub>-NLS. We were able to clearly observe mitochondria present in the nucleus of cells, as indicated by 3D reconstruction (Fig.4A, Movie S5). In addition, cytoplasmic components within the nucleus were visible in knockdown cells by TEM (Fig.4B, i and ii). These structures do not represent nuclear invaginations since they lack the double membrane with ribosome decoration that characterizes the NE (Fig.4B, iii). Although we cannot exclude the possibility that some of these organelles are trapped during NE reformation after mitosis, it is unlikely that this is the case as nuclear envelope formation membrane recruitment to chromatin happens during a highly compacted chromatin state with ER membrane tubules being recruited to and flattening directly on the chromatin surface.<sup>20,87</sup> To that end, attempts to physically drag mitochondria into the nucleus during NEF by tagging mitochondrial membrane proteins with chromatin binding domains failed to cause nuclear entrapment (data not shown). Our observations of mitochondria and other cytoplasmic organelles in cells with a high frequency of NERDI are consistent with results from a recent study of laminopathy cells that also found intranuclear mitochondria associated with interphase NE rupturing.<sup>89</sup> The movement of organelles into the nucleus could have severe consequences for the cell since structures of this size are likely to be trapped inside the nucleus for the duration of interphase.

## Discussion

The NE partitions the eukaryotic cell into two compartments between which there is a highly regulated exchange of proteins, nucleic acids, and cellular activities. With the delineation of specific cellular processes to distinct and separate spaces, spatial regulation is able to add to the complex series of pathways that control normal cellular physiology. Nuclear-cytoplasmic transport, which occurs through the nuclear pore complex, is an important aspect of normal cell function, and defects in this process have been reported in human genetic diseases and in divergent types of cancer.<sup>106</sup> These defects can occur in the signal- transduction pathways that regulate the transfer of factors such as p53 and  $\beta$ -catenin in and out of the nucleus, or in the general nuclear import and export machinery itself.<sup>106</sup> Our results show that the most dramatic example of compromised spatial identity in the cell may well be NERDI. We describe a phenomenon in cancer cells where the interphase NE transiently ruptures, mixing nucleoplasm and cytoplasm. We show that decreased lamin expression leads to localized deformation of the NE that expands and eventually ruptures, leading to the mixing of nuclear and cytoplasmic components and transiently abrogating proper cellular compartmentalization (Fig.4C). Consequences of this event include mislocalization of proteins, changes to the containment of the genome, and the introduction of large cytoplasmic structures into the protected nuclear

space. The uncontrolled movement of macromolecules across a ruptured NE is likely to perturb processes dependent on compartmentalized localization of regulatory proteins such as cell growth pathways, potentially contributing to neoplastic transformation.

Furthermore, nuclear export of properly processed mRNAs is a critical component of eukaryotic gene expression. The complex life cycle of gene transcription products is performed initially in the nuclear interior and then shifted to cytoplasmic space for final translation. This movement of mRNA between cellular spaces is a target of regulation and our demonstration of the mislocalization of proteins involved in mRNA processing poses interesting questions for the study and interpretation of results from mRNA maturation studies. NE rupturing might lead to the efflux of entire mRNP complexes that are not properly spliced and processed, or in RNA processing factors losing proper cellular compartmentalization, possibly resulting in aberrant translation products or degradation of the respective RNAs.

An important consideration in light of this work is the fact that countless studies over the last decades have used cancer cell lines to study the cell cycle, signal transduction pathways and DNA damage and repair. An underlying assumption of all these studies was that the NE breaks down only during mitosis, when the majority of transcription is halted and when chromatin is in a highly compacted state. Realizing that, at least in some of the most frequently used cell lines, the NE transiently ruptures in a small

subset of cells may lead to a new evaluation of previous results. Interphase NE rupturing suggests that additional levels of nuclear-cytoplasmic communications exist and may bring new insights to transcriptional regulation and gene expression studies or other work involving factors with regulated movement between the nuclear and cytoplasmic compartments.

In addition to its role in mediating signal-dependent, active nuclear transport, a long proposed cellular function for the evolution of the NE is to form a protective shield around the nuclear genome and thereby prevent the direct contact between cytoplasmic proteins, organelles, and metabolic by-products and the nuclear DNA. Our findings that organelles and cytoplasmic components can enter the interphase nucleus suggest that, in some cancer cells, eukaryotic cell organization is compromised and may result in insult to the genome. The presence of such components in the nucleus during interphase, when DNA is replicated and transcriptional programs are executed, could be a source of DNA damage that has not yet been appreciated. Cellular organelles such as mitochondria generate a high number of reactive oxygen species that, without the proper machinery present to neutralize them, could induce mutagenesis. Of note, the presence of cytoplasmic structures, including mitochondria, vacuoles and Golgi fragments inside the nuclei of neoplastic cells has been observed repeatedly by EM<sup>107</sup> without a concrete explanation or mechanism for their presence. Furthermore, 'nuclear mitochondria' were observed in lymphoid tumors over

three decades ago,<sup>108</sup> suggesting that this phenomenon might be relevant for tumor formation in vivo. Our results provide a cell biological explanation for the presence of these 'nuclear cytoplasmic bodies'.

Why does NE rupturing in interphase occur in cancer cells but not, or very infrequently, in primary cells? One explanation could be that the mechanical properties of the NE in cancer cells are different from non-cancer cells. For instance, loss of lamin expression or altered lamin structure is often found in cancer cells, including leukemia and lymphoma,<sup>109-111</sup> colon cancer,<sup>112</sup> prostatic cancer,<sup>113</sup> gastric cancer<sup>44</sup> and lung cancer.<sup>45,95</sup> Our data, along with results from other labs and studies of the affect of lamin loss on nuclear elastic properties, indicate that low lamin levels or aberrant lamina organization might make the NE more susceptible to rupture. One striking feature of NE rupturing during interphase is that it is reversible, with cells able to recover and go on to produce progeny. Therefore, a mechanism must be in place to re-seal the double membrane, suggesting that the phenomenon has existed long enough for cells to have adapted a response. This is the first example of a NE repair mechanism outside of mitotic context and underscores the dynamic organization of the NE at a level that has not previously been appreciated.

The failure to properly localize nuclear components as a result of defective nuclear transport has been directly associated with defects in chromatin organization and gene regulation.<sup>106</sup> Since the NE is commonly

thought to remain intact during interphase, all nucleo-cytoplasmic communication is thought to occur through NPCs. The discovery that the NE undergoes transient rupturing during interphase establishes a novel example of aberrant nucleo-cytoplasmic communication that does not depend on trafficking through NPCs. Unlike controlled nuclear-cytoplasmic transport, this loss of the NE barrier function likely represents a catastrophic event that potentially affects the regulation of multiple cellular processes, with apparent changes to the localization of parts of the genome in the extreme cases.

Micronucleation has long been considered to result from imperfect segregation of acentric chromosomal fragments or fragments of overly long chromosomes during karyokinesis.<sup>114,115</sup> A study has previously shown that acentric double minute chromosomes (DMs) can be sorted to the nuclear periphery during S phase and then selectively eliminated from the nucleus by micronucleation in advance of karyokinesis.<sup>116</sup> Our results provide evidence that fragmentation of the nuclear genome may occur in interphase associated with the phenomenon of NE rupturing.

Despite our substantial understanding of molecular mechanisms and gene mutations involved in cancer, the technical approaches for diagnosis and prognosis of cancer are still limited. A deformed and enlarged nuclear morphology is a common characteristic of cancer cells, and the “roundness” of the nucleus is a good indicator to distinguish benign, low grade, and malignant cells.<sup>74</sup> In the clinical setting, the morphology of the nucleus is used

universally for diagnostic and prognostic prediction of malignancies of tumor cells, referred to as “nuclear grade.”<sup>74</sup> Linking cytological information such as aberrant nuclear morphology with functional data (e.g., NE rupturing) could help develop new diagnostic tools or refine existing ones. Our results will increase our understanding of pathological NE organization and might open new avenues for clinical diagnostics.

## **Materials and Methods**

### **Cell culture**

U2OS, HeLa, SJSA and MCF7 cell lines were cultured according to standard tissue culture practices and maintained in the logarithmic phase of growth in DMEM (CellGo) supplemented with 10% fetal bovine serum (HyClone), penicillin, and streptomycin. IMR90 cell line was cultured in DMEM with Glutamax (Gibco) supplemented with 20% fetal bovine serum (HyClone) and non-essential amino acids (CellGo).

### **siRNA transfection**

Cells were transfected twice at 2d and 4d prior to analysis using 0.6ml Lipofectamine 2000 (Invitrogen) with 25–50 nmol of the siRNA oligos: Lamin A/C (UGU UCU UCU GGA AGU CCA GTT), lamin B1 (CGC GCU UGG UAG AGG UGG ATT), lamin B2 (ACU CGG CUU CCU CCU CCU CTT), scrambled

(UAG ACA CCA UGC ACA AUC CTT), LBR, Lap2b, Nup93, and Nup 107 (sequences previously reported).<sup>20,87</sup>

### **Expression constructs**

GFP<sub>3</sub>-NLS was constructed using the Gateway system (Invitrogen) to insert a sequence of tandem EGFPs and the NLS (PPKKKRKV) from the SV40 large T antigen into the N-terminal cycle3-GFP containing vector, pcDNA6.2/DEST53. FLAG-Vpr was a generous gift of Warner Greene (UCSF, San Francisco, CA, USA,) H2B-mCherry and GFP-IBB were generous gifts of Michael Schmitz and Daniel Gerlich (ETH, Zurich, Switzerland). The mCherry-lamin B2 construct was made by inserting full-length lamin B2 (a gift from Harald Hermann, DKFZ, Heidelberg, Germany) into mCherry-DEST vector (a gift from Clodagh O'Shea, the Salk Institute, La Jolla CA, USA). Sec61 $\beta$ -GFP was previously reported. mCherry-tubulin was a generous gift from Chris Somerville (UC Berkeley, Berkeley CA, USA). pTurboRFP-Mito was purchased from Evrogen.

### **Stable cell lines**

The lamin B1 shRNA stable cell line was generated by first transiently transfecting GFP<sub>3</sub>-NLS into U2OS cells and selecting with G418 after 48 h. Cells were propagated for 2 weeks under G418 selection and then the GFP+ population collected by FACS. The GFP+ population was then infected with lenti-viral particles carrying a pLKO.1 plasmid containing an shRNA directed

against lamin B1 (OpenBiosystems) and selected after 48 h with puromycin. Cells were carried in both selective markers for 6 passages and stocks frozen. Cells were maintained in both selection markers for the duration of imaging experiments.

### **Immunofluorescence and protein gel blot antibodies**

Primary antibodies used in this study are: rabbit  $\alpha$ -eIF4AIII and rabbit  $\alpha$ -UPF1 were kind gifts from Jens Lykke-Andersen, UC San Diego, La Jolla, CA USA, rabbit  $\alpha$ -lamin A (Sigma), goat  $\alpha$ -lamin B1 (Santa Cruz), mouse  $\alpha$ -lamin B2 (Abcam), rabbit  $\alpha$ -FLAG (Cell Signaling), and mouse  $\alpha$ -tubulin (Sigma). Secondary antibodies are, from Invitrogen: goat  $\alpha$ -mouse Alexa Fluor 488, goat  $\alpha$ -rabbit Alex Fluor 488, donkey  $\alpha$ -goat Alexa Fluor 488, goat  $\alpha$ -mouse Alexa Fluor 568, goat  $\alpha$ -rabbit Alexa Fluor 568, goat  $\alpha$ -mouse Alexa Fluor 647, goat  $\alpha$ -rabbit Alexa Fluor 647, and donkey  $\alpha$ -goat Alexa Fluor 647; and from Li-Cor: goat  $\alpha$ -mouse IRDye 680, goat  $\alpha$ -rabbit IRDye 680, donkey  $\alpha$ -goat IRDye 680, donkey  $\alpha$ -mouse IRDye 800, and donkey  $\alpha$ -rabbit IRDye 800.

### **Protein gel blotting and whole cell lysates**

Whole cell lysates were collected at 70–90% confluency by washing twice in PBS, scraping in lysis buffer, and protein concentration normalized using BCA Protein Assay kit (Pierce). MDAMB, HCC and HMEC lysates were a generous gift from Clodagh O'Shea, the Salk Institute, La Jolla, CA, USA.

Protein gel blotting was performed using the indicated primary and secondary antibodies. Blots were analyzed on the Li-Cor Odyssey system and processed using Photoshop CS5 extended (Adobe).

### **Live and confocal imaging**

Live-imaging was performed in 8 well m-slide chambers (iBidi) on either a Yokagawa spinning disk built around a Leica DMRIE2 inverted confocal microscope with a 20x air or 63x 1.4NA oil immersion objective at 37°C maintained by a CO<sub>2</sub> enriched air stream incubator (Solent Scientific) and images captured with an EM CCD (Hamamatsu) using SimplePCI software (Compix) or on a Zeiss/Yokagawa spinning disk inverted confocal microscope with a 20x air or 63x 1.4NA oil immersion objective at 37°C maintained by a CO<sub>2</sub> enriched air stream incubator (Pecon) and images captured with an EM CCD (Hamamatsu) using AxioVision software (Zeiss). For fixed imaging, cells were grown on glass coverslips and images were acquired on either a Leica SP2 scanning confocal microscope with a 63x 1.4NA oil immersion objective with LCS software (Leica), or on a Zeiss LSM 710 scanning confocal microscope with a 63x 1.4NA oil immersion objective with Zen software (Zeiss). Fluorochromes and stains used in this study are EGFP, cycle3GFP, mCherry, Alexa Fluor 488, Alexa Fluor 568, Alexa Fluor 647, Hoechst 33342 (Molecular Probes), and MitoTracker Red CMXros (Invitrogen).

## **Electron microscopy**

Cells were grown in 35mm plastic culture dishes were fixed using the protocol of Gilula et al. (1978).<sup>117</sup> The cells were fixed in 2.5% glutaraldehyde in 0.1M Na cacodylate buffer (pH7.3), buffer washed and fixed in 1% osmium tetroxide in 0.1M Na cacodylate buffer. They were subsequently treated with 0.5% tannic acid followed by 1% sodium sulfate in cacodylate buffer and then dehydrated in graded ethanol series. The cells were cleared in HPMA (2-hydroxypropyl methacrylate: Ladd Research) and embedded in LX112 resin. Following overnight polymerization at 60°C, small pieces of resin were attached to blank blocks using SuperGlue (Scotch). Thin sections (70nm) were cut on a Reichert Ultracut E (Leica) using a diamond knife (Diatome, Electron Microscopy Sciences), mounted on parlodion coated, copper, slot grids and stained in uranyl acetate and lead citrate. Sections were examined at 80kV on a Philips CM100 TEM (FEI) and data documented on a Megaview III CCD camera (Olympus Soft Imaging Solutions).

## **Image processing and data analysis**

Images were analyzed and processed for display using Photoshop CS5 extended (Adobe). Spilling frequency was determined using a MatLab (Mathworks) nuclei counting algorithm to count total number of cells, movies were then analyzed manually, frame by frame, for interphase nuclear ruptures. The number of times each cell ruptured was also tabulated and the average

of this number used to determine the frequency of ruptures within individual cells. Statistics were performed using either Prism 5 (GraphPad) or Excel 2011 (Microsoft). Curve fitting of rupture dynamics was done using Prism 5 (GraphPad) as described in the text.

### **3D reconstruction**

Optimized confocal z-series were acquired on a Zeiss LSM 710 scanning confocal microscope and assembled into 3D surfaces for each channel by absolute intensity and with thresholding adjusted so that generated surfaces are matched to fluorescence signal using Imaris (BitPlane).

### **Supplementary Material**

Supplementary Figures S1–S3 and Supplementary Movies S1–S5 may be downloaded here: <http://www.landesbioscience.com/journals/nucleus/article/18954/>

### **Acknowledgments**

Chapter III, in full, consists of the following publication:

Vargas JD, Hatch EM, Anderson DJ, Hetzer MW. 2012. Transient nuclear envelope rupture during interphase in human cancer cells.

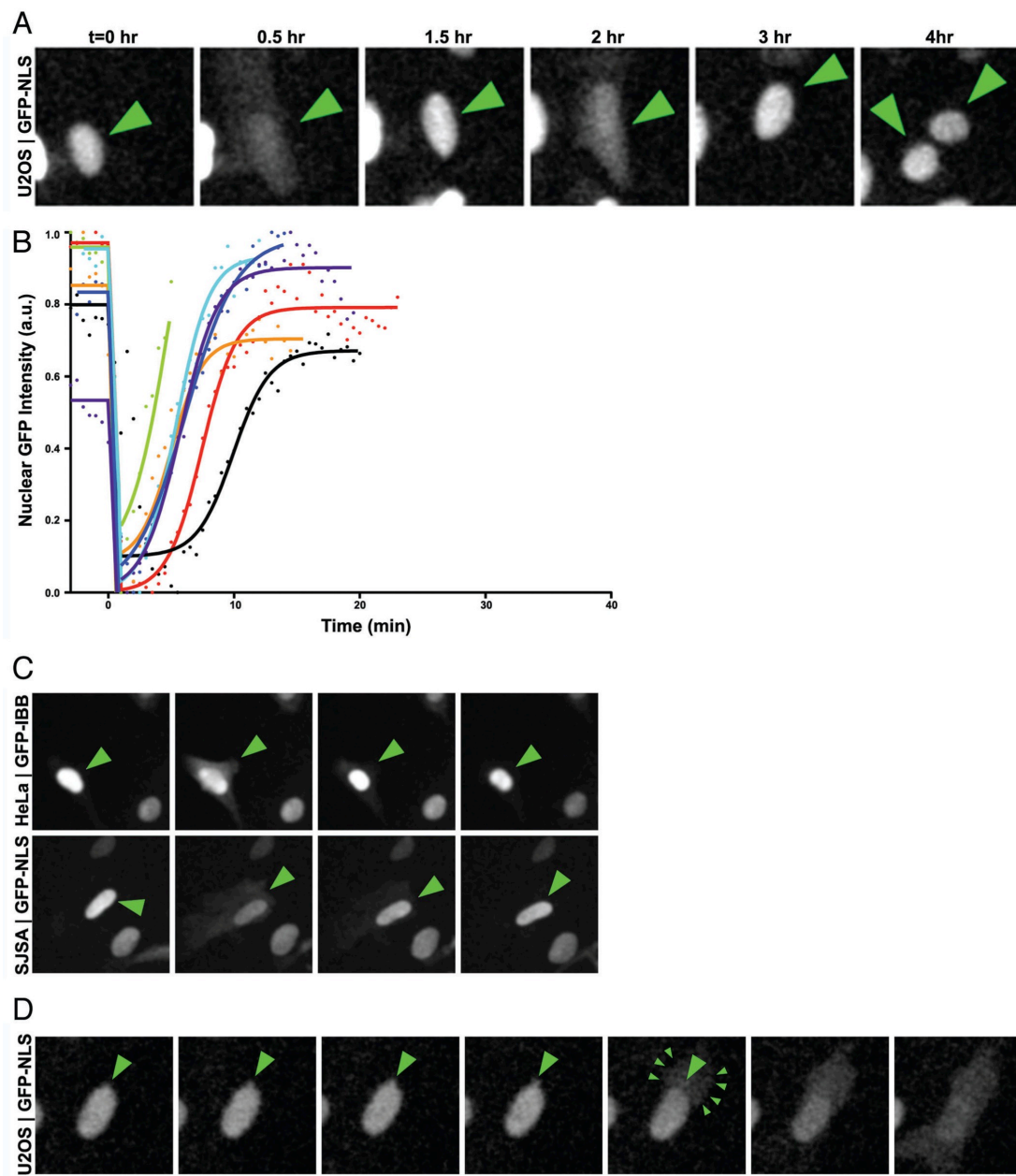
Nucleus 3(1):14-21

I was the primary researcher and author of these studies under the supervision and direction of Martin Hetzer. Emily Hatch contributed experimental work to this study. Daniel Anderson developed imaging assays and analysis methods for this study.

The authors would like to thank Malcolm Wood, James Fitzpatrick, and Matthew Joens for their expertise in EM, the Waitt Center for Advanced Biophotonics for their expertise, and members of the Hetzer laboratory for critically reading the manuscript.

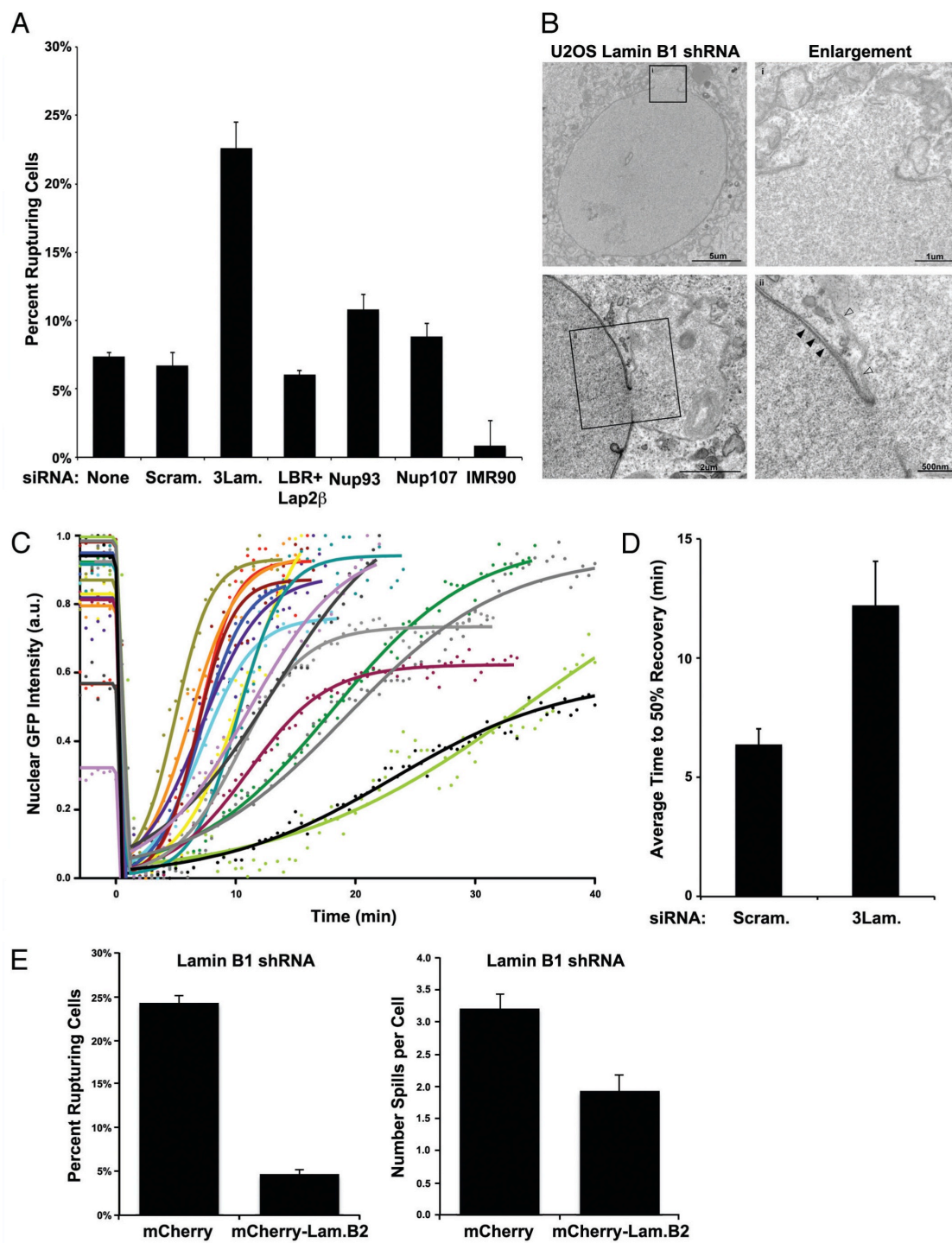
**Chapter III Figure 1: Nuclear envelope rupture during interphase.**

(A) U2OS cells transiently transfected with GFP<sub>3</sub>-NLS and imaged every 3 min for 36 h show transient interphase rupturing of the NE followed by recovery of GFP<sub>3</sub>-NLS into the nucleus. (B) Dynamics of a rupture event. U2OS cells expressing GFP<sub>3</sub>-NLS were imaged every 30s to capture NERDI in high temporal resolution. GFP intensity was normalized by setting the maximum and minimum intensity for each cell to 1 and 0, respectively. Curve fittings of individual interphase NE ruptures were plotted (lines) along with raw data (points). Data was fit using the equation:  $Y = IF(X, X_0, Y_0, IF(X, X_1, Y_0 - S \cdot X, Bottom + (Top - Bottom) / (1 + 10^{((\text{Log}50 - X) \cdot \text{HillSlope}))))$  where:  $X_0$  is the point of inflection between the plateau and the spilling event,  $Y_0$  is the plateau value,  $X_1$  is the initial point of recovery,  $S$  is the slope of spilling,  $Bottom$  is the lower plateau for recovery,  $Top$  is the upper plateau of recovery,  $\text{Log}50$  is the point of 50% recovery, and  $\text{HillSlope}$  is the linear rate of recovery. (C) Representative images of HeLa cervical and SJSA osteosarcoma cancer cell lines demonstrating spilling in diverse cancer cell types. (D) U2OS cells transiently transfected with GFP<sub>3</sub>-NLS and imaged every 3 min show localized nuclear deformation and cytoplasmic GFP signal originating from the site of deformation.



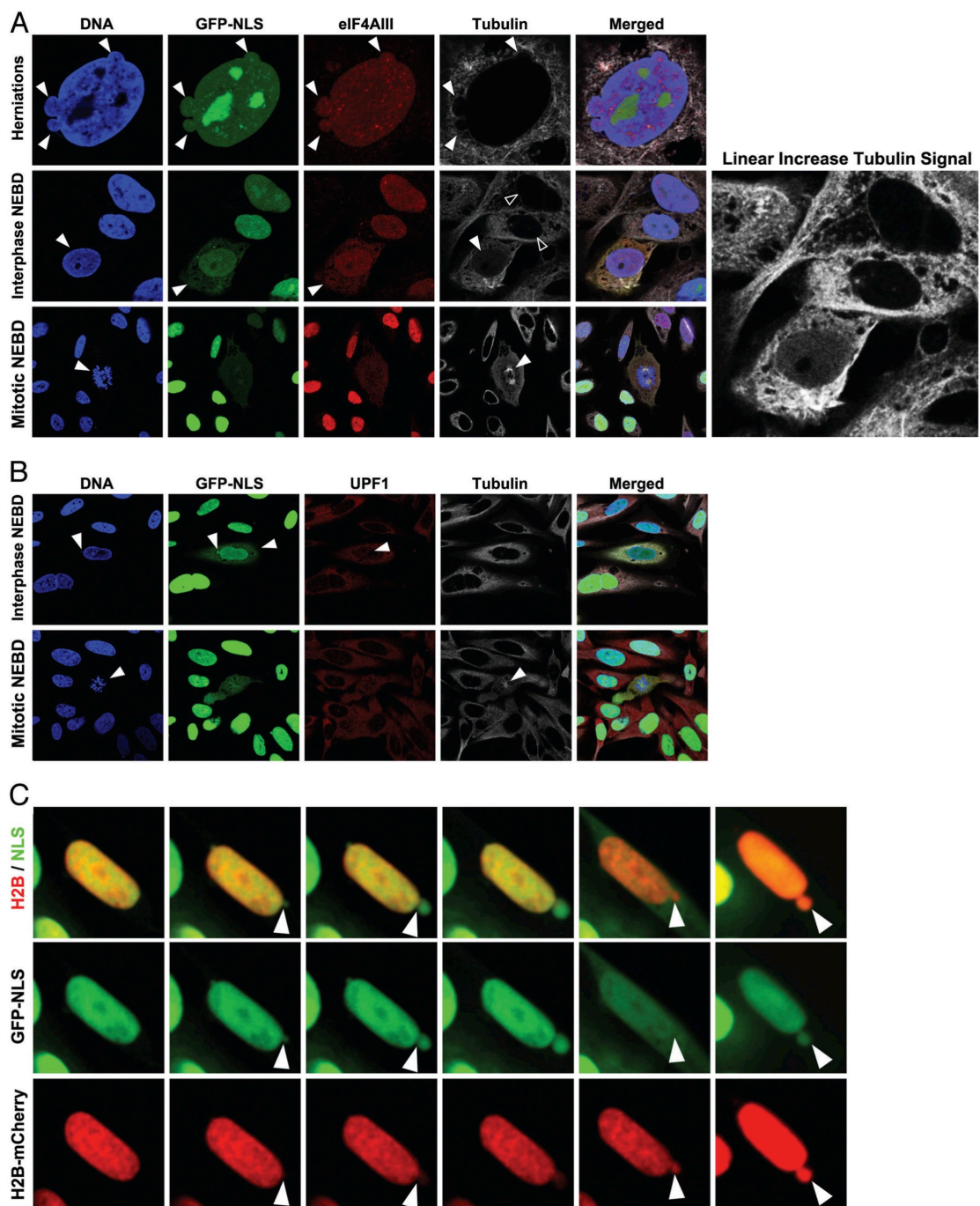
**Chapter III Figure 2: Reduced lamin levels accentuate nuclear ruptures.**

(A) Frequency of NERDI in U2OS cells after treatment with two rounds of knock down by siRNA directed against: the 3 lamin genes, LBR and Lap2 $\beta$ , Nup93, or Nup107, compared with reporter only (none), scrambled siRNA, or non-transfected IMR90 controls ( $p = 0.02$  3LamKD vs Scram. siRNA). Cells were imaged for a period of 36 h and frequencies represent the proportion of cells that experience an interphase NE rupture at least once over the course of the experiment. (B) Transmission electron microscopy (TEM) of U2OS stably reduced for lamin B1 expression by shRNA and stained with tannic acid to enhance lamin visualization (solid arrows). Characteristic NE herniations exhibit reduced tannic acid staining (open arrows). (C) Dynamics of a rupture in U2OS cells treated with 3 lamin siRNA. U2OS cells transfected with GFP- NLS and 3 lamin siRNA pool were imaged every 30s to capture NERDI in high temporal resolution. Curve fittings, as in Figure 1B, of individual interphase NE ruptures are plotted (lines) along with raw data (points) and show the dynamics of the event. (D) Recovery half-lives of rupture were obtained from each curve and averaged for control and 3 lamin siRNA treated cells with measured half-lives of ~6 and ~12 min, respectively. (E) Left: U2OS cells stably reduced for lamin B1 expression by shRNA and expressing the GFP<sub>3</sub>-NLS reporter were transiently transfected with either mCherry alone or human lamin B2 tagged with mCherry (mCherry-LmnB2). Frequency of NERDI was analyzed in transfected cells imaged for 36 h. Cells with mCherry-LmnB2 aggregates were excluded from analysis. Right: Average number of spills per cell was determined for cells transfected with either mCherry or mCherry-LmnB2 and imaged for 36 h. For both,  $n \geq 340$  cells over 2 experiments. Error bars are standard error and the difference in percent cells with spilling nuclei is significant ( $p \leq 0.01$ ) by Student's t-test.



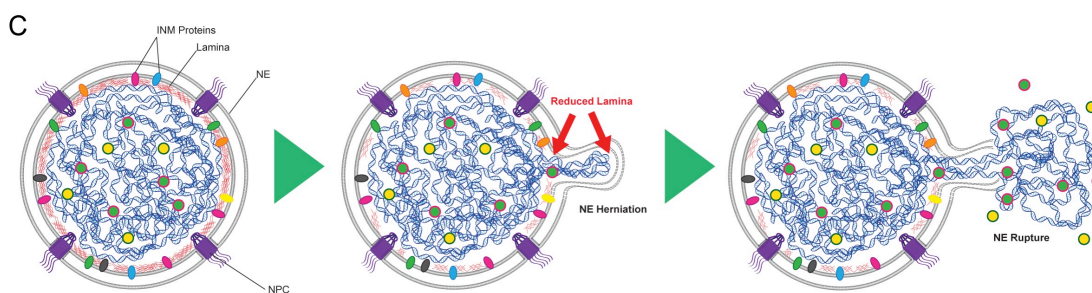
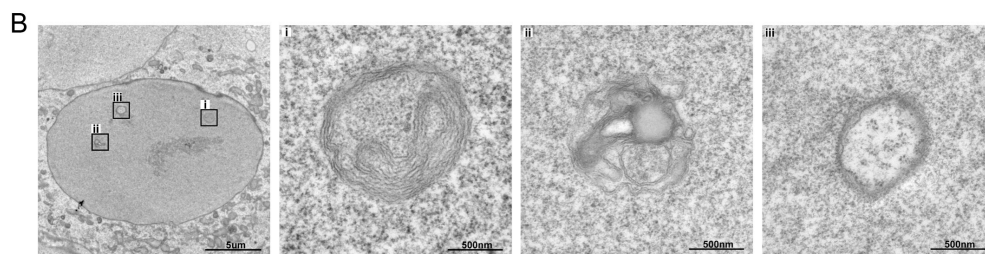
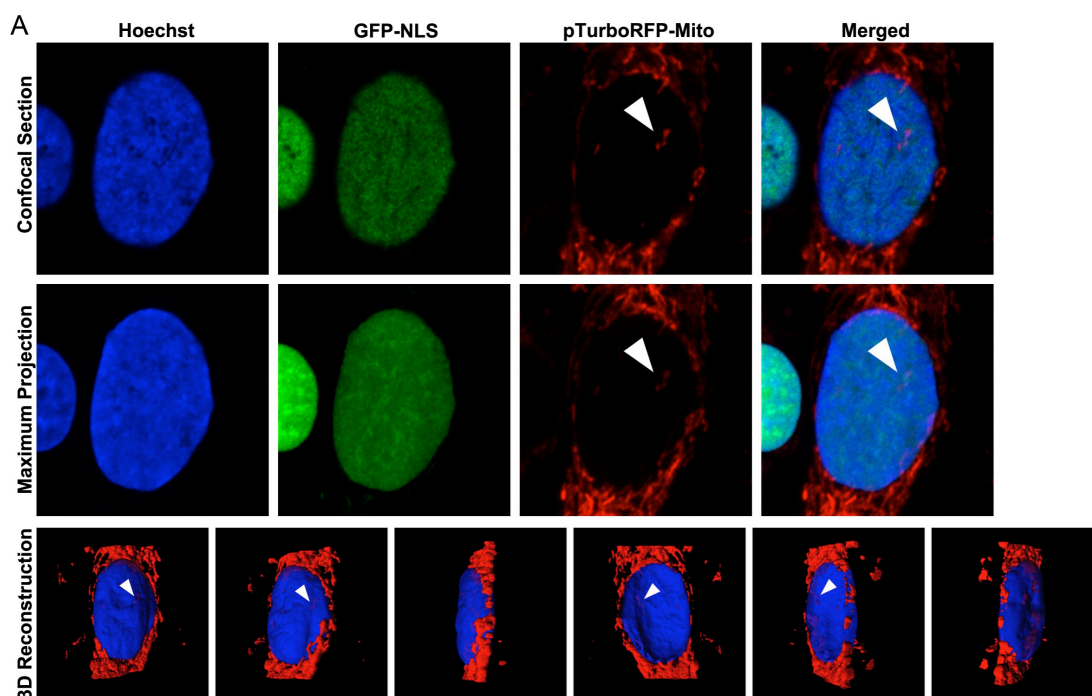
**Chapter III Figure 3: Mislocalization of nuclear and cytoplasmic components.**

(A) U2OS cells stably reduced for lamin B1 expression by shRNA, expressing GFP<sub>3</sub>-NLS reporter and stained with antibodies against eIF4AIII (red), tubulin (white), and for DNA with Hoechst (blue) show characteristic NE herniations (top arrows), and cytoplasmic localization of eIF4AIII during an interphase NE rupture (middle panel, arrows) with corresponding nuclear influx of soluble tubulin (middle, solid vs. open arrows) contrasted from mitotic NEBD with characteristic condensed DNA and tubulin spindle (bottom panel, arrows). Zoom panel shows linear brightness increase for visualization of diffuse nuclear tubulin. (B) U2OS cells treated as in part A stained for UPF1 (red) and tubulin (white). UPF1 is present in the nuclear interior during an interphase rupture event (top panel, arrows) contrasted from mitotic NEBD by chromatin structure and mitotic spindle (bottom panels, arrows). (C) Time series images of NERD1 in U2OS cell showing NE deformation and rupture and chromatin dynamics during the event. Nuclear integrity was monitored with GFP<sub>3</sub>-NLS (green) and chromatin with H2B-mCherry (red) reporters. GFP<sub>3</sub>-NLS diffuses throughout cytoplasm during NE rupture; H2B-mCherry spills into cytoplasm but is contained to a localized area just beyond the NE boundary.



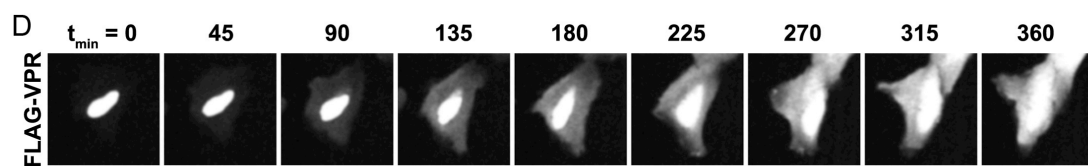
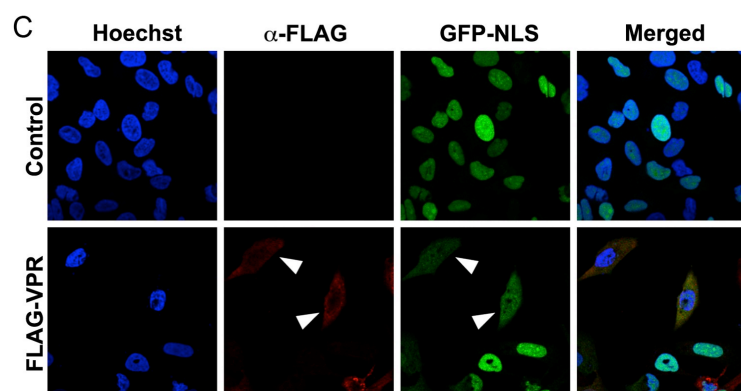
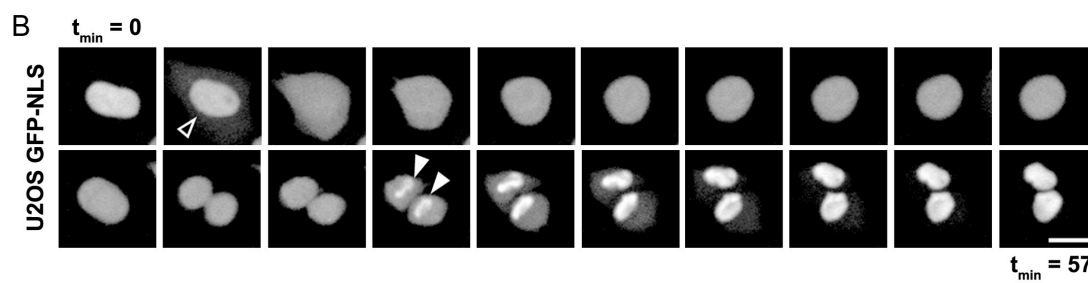
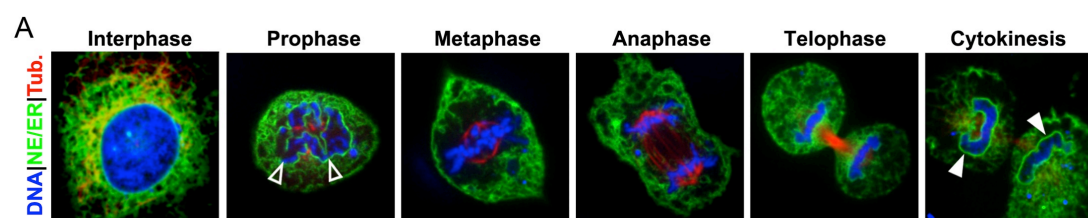
**Chapter III Figure 4: Consequences of interphase nuclear rupture.**

(A) U2OS cells expressing GFP<sub>3</sub>-NLS (green) and pTurboRFP-mito (red), and stained for DNA with Hoechst (blue) show nuclear mitochondria in confocal slice (top), maximum intensity projection (middle) and 3D reconstruction with nuclear mitochondria indicated (arrows). (B) TEM of U2OS cells stably reduced for lamin B1 expression by shRNA showing cytoplasmic bodies enclosed within the nucleus (i and ii) contrasted from nuclear invaginations with characteristic NE double membrane and ribosome decoration (iii). (C) Proposed model for Nuclear Envelope Rupture During Interphase (NERDI) in cancer cells. Reduced lamin expression leads to a weakened NE that distends outward, eventually rupturing with a mixing of nuclear and cytoplasmic components.



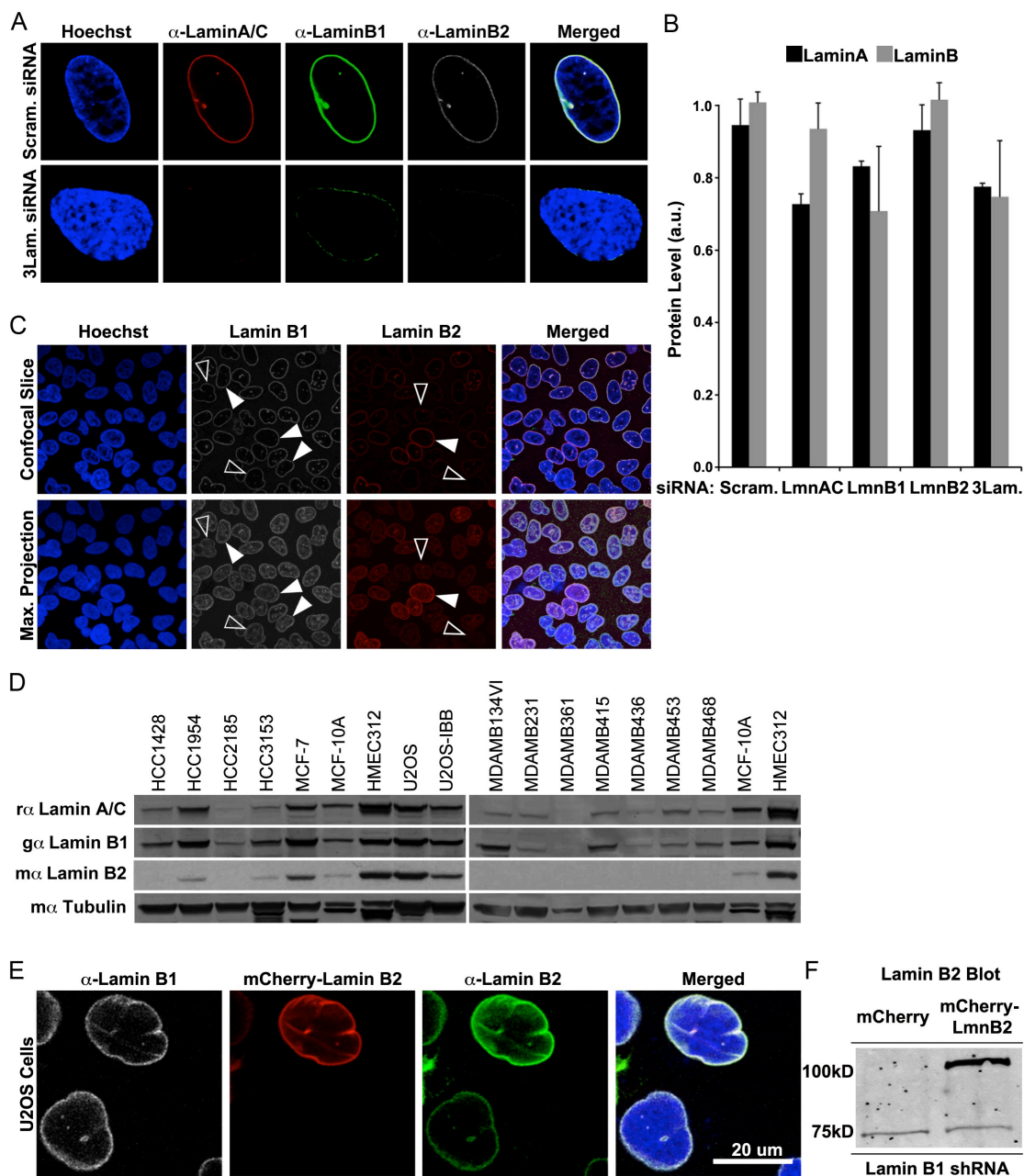
**Chapter III Supplemental Figure 1: GFP<sub>3</sub>-NLS Expression & Localization.**

A) Phases of the cell cycle. Freeze frame images from live imaging of U2OS cells expressing a fragment of Sec61 $\beta$ -GFP (green) to visualize the NE/ER, mCherry-tubulin (red), and stained for DNA with Hoechst (blue) show mitotic NEBD (open arrows) and nuclear envelope reformation (solid arrows). B) Freeze frame images from live imaging of U2OS cells expressing GFP<sub>3</sub>-NLS showing mitotic NEBD (open arrows) and re-accumulation of GFP<sub>3</sub>-NLS after nuclear envelope reformation (solid arrows). C) Immunofluorescence images of untransfected (top) and FLAG-VPR transiently transfected U2OS cells expressing GFP<sub>3</sub>-NLS stained for the FLAG epitope (red) demonstrate cytoplasmic localization of GFP<sub>3</sub>-NLS in cells expressing FLAG-VPR. D) Freeze frame images from live imaging of U2OS cells expressing GFP<sub>3</sub>-NLS and transiently transfected with FLAG-VPR show NE rupture persisting for 300 minutes without recover of GFP<sub>3</sub>-NLS into the nucleus.



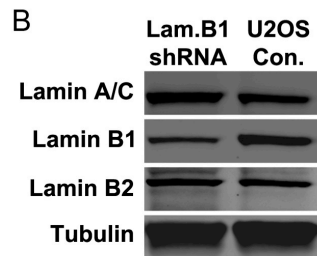
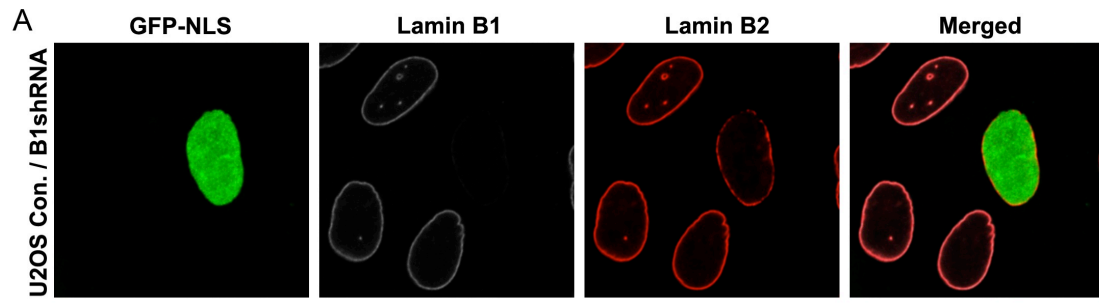
**Chapter III Supplemental Figure 2: Lamin Knock Down and Differential Expression.**

A) Immunofluorescence of U2OS cells treated with scrambled control or 3 lamin siRNA cocktail showing knock down efficiency of lamins A/C (red) B1 (green) and B2 (white) when siRNAs are delivered as a pool by transient transfection. B) Analysis of western blots of U2OS whole cell lysates from cells treated with individual siRNAs against lamin A/C, B1, or B2 and the combination of the 3 siRNAs delivered as a pool by transient transfection show an average reduction of 20% of lamin protein expression across a population of cells in culture. C) Differential expression of lamin protein in U2OS cells demonstrated by immunofluorescence of U2OS cells stained for lamins B1 (white) and B2 (red). Confocal slice (top) and maximum projections (bottom) show different intensities between cells for both b-type lamins, indicated by arrows. D) Western blot of whole cell lysates from 12 breast cancer cell lines (HCC, MCF-7 and MDAMB lines) compared to untransfected U2OS osteosarcoma lines, U2OS stable line expressing the integrity reporter GFP-IBB, MCF-10A spontaneously immortalized line, and HMEC312 primary cell line show diverse levels of expression of the three lamin proteins. E) Normal U2OS cells stained for endogenous lamin B1 (white) and B2 (green) expression and for DNA (blue) transiently transfected with an mCherry-lamin B2 expression construct (red) showing localization of the full length lamin B2 construct and the endogenous b-type lamin proteins. F) Western blot showing expression of mCherry-lamin B2 in U2OS cells stably reduced for lamin B1 expression by shRNA compared to controls transfected with mCherry.



**Chapter III Supplemental Figure 3: shRNA Stable Lamin Knock Down.**

A) Immunofluorescence of U2OS cells stably expressing GFP<sub>3</sub>-NLS (green) and an shRNA against lamin B1, showing lamin B1 (white) and lamin B2 (red) expression. B) Western blot of lamin B1 shRNA knock down efficiency showing lamin A/C, lamin B1, and lamin B2 protein expression with tubulin as a loading control.



**Chapter III Supplemental Movie 1: Nuclear envelope rupture during interphase.**

U2OS cells expressing GFP<sub>3</sub>-NLS were imaged over time and show the rapid loss of nuclear GFP intensity into the cytoplasm with a slower recovery of nuclear signal and concomitant clearing of cytoplasmic GFP.

**Chapter III Supplemental Movie 2: Rupturing appears heritable and recoverable.**

U2OS cells expressing GFP<sub>3</sub>-NLS stably reduced for lamin A/C, B1, and B2 expression by triple siRNA spill frequently, recover, and go on to divide with progeny also exhibiting interphase NE rupturing.

**Chapter III Supplemental Movie 3: Rupturing of nuclei produces micronuclei-like bodies.**

U2OS cells from Movie 2 above shown through an interphase rupture event and cell division have associated extra-nuclear spheres containing GFP<sub>3</sub>-NLS.

**Chapter III Supplemental Movie 4: Localized nuclear herniation precedes rupturing.**

U2OS cell expressing GFP<sub>3</sub>-NLS is shown during a rupture event. The movie is slowed for facilitated visualization of the nuclear herniation.

**Chapter III Supplemental Movie 5: Nuclear mitochondria.**

3D reconstruction of a U2OS cell stably reduced for lamin B1 expression by shRNA and expressing pTurboRFP-Mito show the presence of mitochondria within the DNA.

Chapter IV

Conclusion

In this thesis several areas related to the biogenesis, structural integrity and barrier function of the metazoan nucleus were examined. The aim of this chapter is to summarize key findings of my thesis and discuss these results in the context of recent advances in the field and the potential insights these results bring to cell biology.

### **DNA/chromatin interacting membrane proteins of the INM role in post-mitotic reformation of the NE**

The aim of chapter II was to identify and characterize proteins that drive membrane targeting to and spreading around the chromatin masses that will become the daughter nuclei of newly formed cells post-mitosis. At the time, the recent identification of a family of membrane curving proteins that act as negative regulators to NEF, the reticulons, created the immediate question: if these are negative regulators, what players are actually driving the process? We hypothesized, supported by postulation in the primary literature, that transmembrane proteins that have the capacity to bind or interact with DNA/chromatin and that are found in the interphase NE may play a key role in the physical juxtapositioning of ER membranes to the chromatin masses at the end of mitosis thus driving the reformation process. Further, we reasoned that such chromatin interaction domains, present in so many diverse proteins, could be indicative of a novel mitotic function for many known proteins, e.g.

coating of the chromatin masses and sealing of the emergent NE. The current questions in the field revolve around the nature of the mitotic ER network. Several publications have focused on the cisternae of the mitotic ER, its proximity to the emerging NE, and the localization of reticulons during reformation. While compelling, each of these reports fails to exclude the model proposed here, wherein reticulons are displaced by lateral diffusion in the ER membrane bilayer to allow a transition from tubule to sheet at the chromatin surface. 3D studies in our lab have shown tubules as the initial contact points of the mitotic ER on chromatin, followed by a collapsing of contacting tubules on the chromatin surface. While the structural nature of the ER membranes contributing to NE formation was not a primary focus of my work, and while the core finding of the role membrane-chromatin tethering plays in the process is not controversial, it is clear that questions remain about the membrane source of the NE. Below I summarize the key findings of this portion of my thesis.

## **Key findings of chapter II**

### **Functionally distinct proteins are co-opted for NE formation at the conclusion of mitosis**

We identified a class of functionally distinct transmembrane proteins of the NE, each with diverse and often unrelated interphase functions, that play a

redundant role in post-mitotic nuclear membrane assembly. When the concentration of one of these proteins is reduced, the rate of NE formation occurs for the most part normally, although at a slower rate. Over 40 transmembrane proteins of the NE contain either putative or confirmed DNA and/or chromatin interaction domains. Our results have shown every such protein tested to be a contributor to the process. If we extrapolate from our small study to assume that most if not all of these proteins similarly contribute, then it is clear evolution has provided for a highly robust system for the re-establishment of the nuclear compartment. Such a level of redundancy is rare in biological systems, and the efficacy of such a system is evidenced by the fact that in our manipulations of protein expression levels we were never able to effectively block the process.

### **Aggregate expression level of membrane-chromatin tethers controls the rate of post-mitotic NE formation**

The increased expression of individual NE-membrane proteins is able to accelerate NE formation, suggesting that binding sites on chromatin are present in excess on the chromatin surface, and that the aggregate sum of the concentrations of the individual players is the primary source of rate limitation. Together with the reticulon family of proteins, nature seems to have setup a balance between NE promoting and NE inhibiting species. The

reason for such a system is not clear, however, similar NE formation times in various cell types indicate this balance is likely a conserved feature, alluding to an evolutionary advantage to achieving proper NE formation timing in this manner.

### **Regulation of NE formation timing is critical for proper cell division processes**

Artificially accelerating the rate of NE formation causes a specific defect in chromosome segregation wherein emergent nuclei are not adequately distanced, in extreme cases resulting in chromatin connections remaining between the daughter nuclei. This suggests that the speed of post-mitotic nuclear assembly is important for the proper partitioning of the genome during cell division.

### **A fundamental step of cellular division can be accelerated by altering gene expression level**

Our results indicate the over expression of INM proteins can accelerate the portion of the cell cycle where the NE is reformed. In human cancer, a myriad of mutations and/or changes in gene expression have been identified that are thought to give cancer cells a growth advantage. Interestingly, several INM proteins have an increased expression level in cancer. The

questions arise, what is driving the change in expression level in cancer, whether such increases in INM protein expression contributes to the rapid growth of cancer cells or whether the specific acceleration of the nuclear assembly process and resultant chromosome segregation defects could contribute to genomic instability. Increasing interest on the NE and its connections to cancer biology is clear from the recent flurry of reviews and primary literature reports on the topic. Since one of the defining features of neoplastic transformation is uncontrolled and often rapid cellular growth, our findings of how cells achieve a critical part of the growth and division process, and that this step can be accelerated by expression level changes, may shed new light on our understanding of human disease.

**NERDI: characterization of a previously unknown phenomenon in human cancer cells**

In this Chapter III of my doctoral work, we identify and characterize a phenomenon that is both peculiar and shocking. During live imaging mitotic assays, we employed a nuclear import reporter that allowed us to monitor the integrity of the NE over time. This was done in order to accurately time mitotic events. Normally the NE is disassembled during the prophase to metaphase transition, allowing the nuclear reporter to flood the cell body. This event is followed by the various mitotic processes and culminates in the re-import of

the nuclear reporter into the nuclei of two newly formed daughter cells. Over the course of several hundred imaging runs, however, we encountered an unexplained behavior with our nuclear reporter. In a small subset of cells, efflux of the nuclear reporter was not followed by a mitotic cycle and production of two cells, rather the reporter was re-accumulated into the nucleus without a division cycle. Upon further investigation of this phenomenon, we found it to occur in several human cancer cell lines and to be linked to altered structural integrity in those cells. The novel finding that regulation of nucleo-cytoplasmic trafficking is not absolute during interphase in cancer cells has important implications for the study of cancer biology and the transformation of basic cell functions in the disease state. That these cancer cells have been examined for decades by hundreds of researchers makes seeing something so visually stunning, with nuclear contents exploding out of the nucleus into the cytoplasmic space before being reincorporated into the nucleus, a rare discovery. Recent intensified interest in the nucleus as it relates to cancer biology and disease is evidenced by 2 reviews in January of 2012 addressing the topic specifically. Our results should put the integrity of the nuclear space at the forefront of such conversations going forward. Moreover, with recent mechanistic insights in the lab showing the role of the connection to the cytoskeleton on ruptures, namely the ability of cytoskeleton inhibitors such as cytochalasin to virtually eliminate NERDI, even in cells where the lamins have been stably reduced,

nuclear rupture biology may be of therapeutic interest. To that end, when we treat cells to arrest rupturing we are able to visualize a drastic decrease in the high level of gH2AX staining seen in high NERDI frequency cells (Fig. 1). Results such as this suggest the initial findings of this study will become more relevant to cancer biology as future studies are carried out linking the phenotype to cancer related phenomena such as DNA mutation, genomic instability and metastasis.

### **Key Findings of Chapter III**

#### **Nuclei of several commonly used human cancer cell lines transiently rupture during interphase**

Using live-imaging approaches we were able to reveal that transient rupturing of the NE occurs in the HeLa, SJSA, and U2OS human cancer cell lines. We show that the rupture of the nucleus is a rapid event, with efflux of the nuclear reporter spreading throughout the cell body within a few minutes. The onset of recovery is immediate, however the complete recovery process is on the timescale of half hours, not minutes. The presence of rupturing in cancer cells of cervical and bone origin suggests that ruptures are not specific to cancer type, but may be a more general characteristic of cancer.

### **Frequency of interphase rupture is linked to the expression level of structural proteins of the NE**

The finding that number of cells within a cancer cell population that exhibit interphase ruptures can be increased by reducing the level of nuclear lamins is important for two reasons. First it indicates that the rupture is likely a structural defect of the nucleus, this is supported by rescue results using expression of a different lamin protein, lamin B2, to mitigate the stable lamin B1 knockdown. Second, because nuclear lamins are reported in numerous studies to be differentially expressed in human cancer, with lower expression often correlating with poor prognosis or highly invasive or metastatic tumors, implicates nuclear rupturing as an important process to consider in advanced lesions. Further the question arises whether decreased expression occurs initially upon transformation to more invasive state, or if such decreased expression might actually drive the change. Interestingly we often see ruptures in cells as they are squeezing between tightly packed cells in an imaging well, suggesting that the more malleable nucleus may allow the cell to be more invasive.

### **Nuclear ruptures are bidirectional with mislocalization of nuclear and cytoplasmic proteins**

During interphase ruptures, both nuclear and cytoplasmic proteins are mislocalized to improper spaces. This finding has implications for the complex process of transcriptional regulation that relies in many ways on sequestering transcription factors in the cytoplasm until appropriate signals are integrated to trigger a transcriptional response. Whether mechanisms that sequester factors in the cytoplasm would prevent complexes from performing transcriptional or other functions in the nucleus is not clear, but is none-the-less an interesting intellectual question. Interestingly, one of the key aspects of cell biology that is spatially separated within cells is the separation of transcription from translation. Normally RNA is produced and processed in the nuclear space before being transported to the ribosome machinery in the cytoplasm for protein production. Nuclear ruptures may lead to an abundance of immature mRNA in the cytoplasm. Without polyadenylation, these transcripts would likely be degraded, however, the effect of such large numbers of unprocessed mRNA in the cytoplasm as could occur during a rupture event has not been investigated. Additionally the knowledge that the maintenance of nuclear and cytoplasmic identities is not absolute may be important for studies using cancer cell lines to study transcription factor localization or activation. Our findings may provide new insights for researchers to consider when investigating nuclear translocation of proteins, especially in the context of cultured cancer cells as an experimental tool for such studies.

### **Nuclear ruptures may impart significant genomic insult and contribute to the mutation capacity of cancer cells**

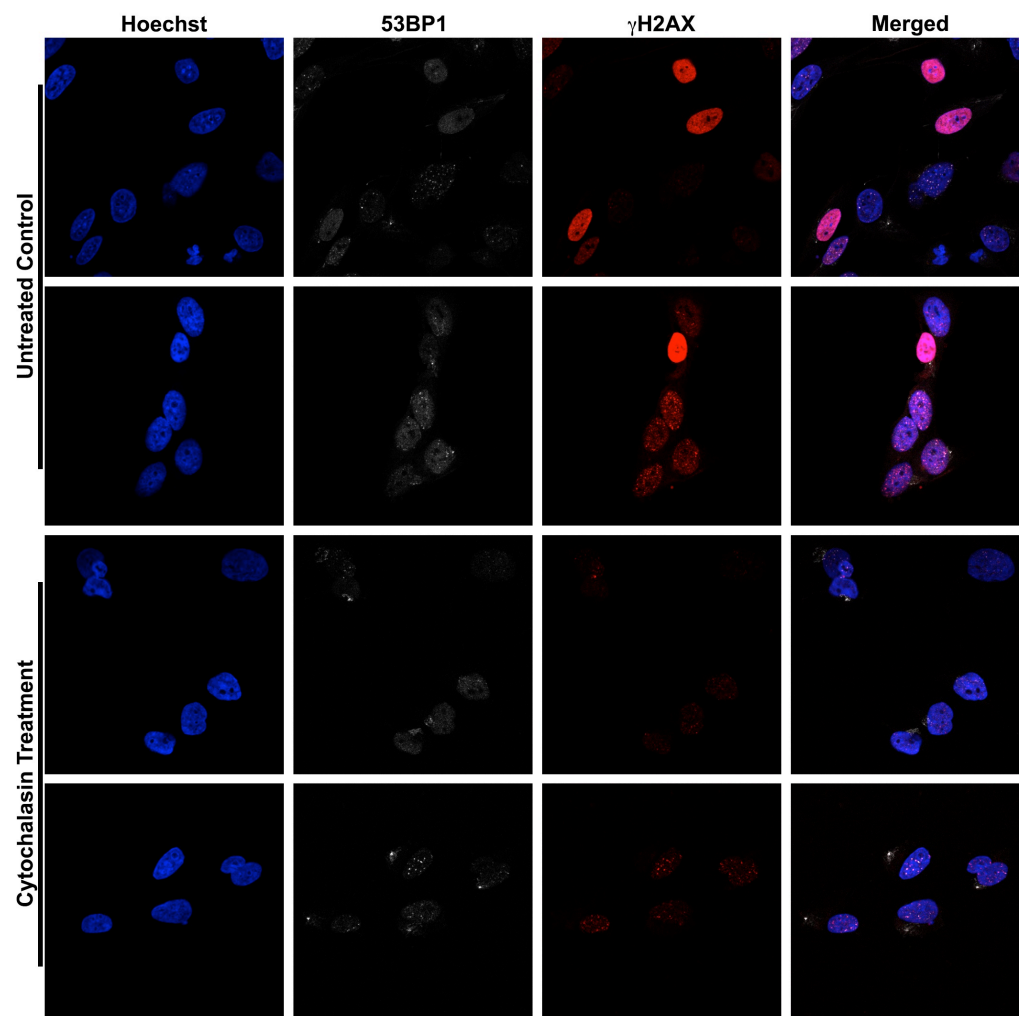
The visualization of genomic material exiting the nucleus during rupture events is profound. The genome normally exists within the protected confines of the nuclear envelope, only exposed to the cytoplasm while in its most compact and transcriptionally inactive state during mitosis. The idea that potentially active chromatin may be exposed to such physical stress during ruptures as to be ejected from the nucleus suggests that rupture events may be a source of mutation. Further, formation of micronuclei like bodies containing nuclear material, as well as the nuclear presence of cytoplasmic bodies in some cells, may also contribute to genomic alterations. These findings highlight NERDI as an important mechanism worthy of further study with regards to cancer biology and many of the transformative processes that contribute to the disease.

### **Acknowledgements**

Chapter IV consists entirely of original text and findings. I was the primary author and contributor to this section.

**Chapter VI Figure 2: Inhibiting NERDI reduces DNA damage staining.**

High NERDI frequency HeLa cells stably reduced for lamin expression were double thymidine blocked and treated with the actin polymerization inhibitor cytochalasin B to decrease rupture frequency. Reducing NERDI decreases the intensity of  $\gamma$ H2AX staining compared to control untreated cells. Of note, control  $\gamma$ H2AX staining is similar to that seen with application of double-strand break DNA damage inducing agents suggestive of significant genotoxic stress abrogation upon actin polymerization inhibition.



## References

1. Watson, M. L. The nuclear envelope; its structure and relation to cytoplasmic membranes. *J Biophys Biochem Cytol* **1**, 257-70 (1955).
2. Gerace, L. & Burke, B. Functional organization of the nuclear envelope. *Annu. Rev. Cell Biol.* **4**, 335-374 (1988).
3. Kite, G. L. The Relative Permeability of the Surface and Interior Portions of the Cytoplasm of Animal and Plant Cells. (A Preliminary Paper). *Biological Bulletin* **25**, 1-7 (1913).
4. Akhtar, A. & Gasser, S. M. The nuclear envelope and transcriptional control. *Nat. Rev. Genet.* **8**, 507-517 (2007).
5. Reddy, K. L., Zullo, J. M., Bertolino, E. & Singh, H. Transcriptional repression mediated by repositioning of genes to the nuclear lamina. *Nature* **452**, 243-247 (2008).
6. Worman, H. J., Ostlund, C. & Wang, Y. Diseases of the nuclear envelope. *Cold Spring Harb Perspect Biol* **2**, a000760 (2010).
7. D'Angelo, M. A., Raices, M., Panowski, S. H. & Hetzer, M. W. Age-dependent deterioration of nuclear pore complexes causes a loss of nuclear integrity in postmitotic cells. *Cell* **136**, 284-95 (2009).
8. D'Angelo, M. A., Gomez-Cavazos, J. S., Mei, A., Lackner, D. H. & Hetzer, M. W. A Change in Nuclear Pore Complex Composition Regulates Cell Differentiation. *Developmental Cell* (2012).doi:10.1016/j.devcel.2011.11.021
9. Crisp, M. *et al.* Coupling of the nucleus and cytoplasm: role of the LINC complex. *J Cell Biol* **172**, 41-53 (2006).
10. Ostlund, C. *et al.* Dynamics and molecular interactions of linker of nucleoskeleton and cytoskeleton (LINC) complex proteins. *J. Cell. Sci.* **122**, 4099-4108 (2009).
11. Padmakumar, V. C. *et al.* The inner nuclear membrane protein Sun1 mediates the anchorage of Nesprin-2 to the nuclear envelope. *J. Cell. Sci.* **118**, 3419-3430 (2005).

12. Aebi, U., Cohn, J., Buhle, L. & Gerace, L. The nuclear lamina is a meshwork of intermediate-type filaments. *Nature* **323**, 560-564 (1986).
13. Beck, M. *et al.* Nuclear pore complex structure and dynamics revealed by cryoelectron tomography. *Science* **306**, 1387-90 (2004).
14. Chook, Y. M. & Blobel, G. Karyopherins and nuclear import. *Curr. Opin. Struct. Biol.* **11**, 703-715 (2001).
15. Marelli, M., Dilworth, D. J., Wozniak, R. W. & Aitchison, J. D. The dynamics of karyopherin-mediated nuclear transport. *Biochem Cell Biol* **79**, 603-12 (2001).
16. Beaudouin, J., Gerlich, D., Daigle, N., Eils, R. & Ellenberg, J. Nuclear envelope breakdown proceeds by microtubule-induced tearing of the lamina. *Cell* **108**, 83-96 (2002).
17. Georgatos, S. D., Pyrpasopoulou, A. & Theodoropoulos, P. A. Nuclear envelope breakdown in mammalian cells involves stepwise lamina disassembly and microtubule-drive deformation of the nuclear membrane. *J Cell Sci* **110 ( Pt 17)**, 2129-40 (1997).
18. Salina, D. *et al.* Cytoplasmic dynein as a facilitator of nuclear envelope breakdown. *Cell* **108**, 97-107 (2002).
19. Anderson, D. J. & Hetzer, M. W. Nuclear envelope formation by chromatin-mediated reorganization of the endoplasmic reticulum. *Nat. Cell Biol.* **9**, 1160-1166 (2007).
20. Anderson, D. J. & Hetzer, M. W. Reshaping of the endoplasmic reticulum limits the rate for nuclear envelope formation. *J. Cell Biol.* **182**, 911-924 (2008).
21. Anderson, D. J. & Hetzer, M. W. Shaping the endoplasmic reticulum into the nuclear envelope. *J. Cell. Sci.* **121**, 137-142 (2008).
22. Lu, L., Ladinsky, M. S. & Kirchhausen, T. Formation of the postmitotic nuclear envelope from extended ER cisternae precedes nuclear pore assembly. *J. Cell Biol.* **194**, 425-440 (2011).

23. Puhka, M., Vihinen, H., Joensuu, M. & Jokitalo, E. Endoplasmic reticulum remains continuous and undergoes sheet-to-tubule transformation during cell division in mammalian cells. *J Cell Biol* **179**, 895-909 (2007).
24. Lu, L., Ladinsky, M. S. & Kirchhausen, T. Cisternal organization of the endoplasmic reticulum during mitosis. *Mol. Biol. Cell* **20**, 3471-3480 (2009).
25. Lu, L. & Kirchhausen, T. Visualizing the high curvature regions of post-mitotic nascent nuclear envelope membrane. *Commun Integr Biol* **5**, 16-18 (2012).
26. Dahl, K. N. *et al.* Distinct structural and mechanical properties of the nuclear lamina in Hutchinson-Gilford progeria syndrome. *Proceedings of the National Academy of Sciences of the United States of America* **103**, 10271-6 (2006).
27. De Sandre-Giovannoli, A. *et al.* Lamin a truncation in Hutchinson-Gilford progeria. *Science* **300**, 2055 (2003).
28. Pollex, R. L. & Hegele, R. A. Hutchinson-Gilford progeria syndrome. *Clin Genet* **66**, 375-81 (2004).
29. Mounkes, L. C. & Stewart, C. L. Aging and nuclear organization: lamins and progeria. *Curr Opin Cell Biol* **16**, 322-7 (2004).
30. Hegele, R. A. The envelope, please: nuclear lamins and disease. *Nat Med* **6**, 136-7 (2000).
31. Nagano, A. & Arahata, K. Nuclear envelope proteins and associated diseases. *Curr Opin Neurol* **13**, 533-9 (2000).
32. Burke, B. & Stewart, C. L. Life at the edge: the nuclear envelope and human disease. *Nat Rev Mol Cell Biol* **3**, 575-85 (2002).
33. Ostlund, C. & Worman, H. J. Nuclear envelope proteins and neuromuscular diseases. *Muscle Nerve* **27**, 393-406 (2003).
34. Muchir, A. & Worman, H. J. The nuclear envelope and human disease. *Physiology (Bethesda)* **19**, 309-14 (2004).

35. Hannen, E. J. *et al.* An image analysis study on nuclear morphology in metastasized and non-metastasized squamous cell carcinomas of the tongue. *The Journal of pathology* **185**, 175-83 (1998).
36. Capo-Chichi, C. D. *et al.* Nuclear envelope structural defects cause chromosomal numerical instability and aneuploidy in ovarian cancer. *BMC Med* **9**, 28 (2011).
37. Caruso, R. A. *et al.* Modifications of nuclear envelope in tumour cells of human gastric carcinomas: an ultrastructural study. *Anticancer Res.* **30**, 699-702 (2010).
38. Maciejczyk, A. *et al.* ABCC2 (MRP2, cMOAT) Localized in the Nuclear Envelope of Breast Carcinoma Cells Correlates with Poor Clinical Outcome. *Pathol. Oncol. Res.* **18**, 331-342 (2012).
39. Agudo, D. *et al.* Nup88 mRNA overexpression is associated with high aggressiveness of breast cancer. *Int J Cancer* **109**, 717-20 (2004).
40. Kinoshita, Y., Kalir, T., Rahaman, J., Dottino, P. & Kohtz, D. S. Alterations in nuclear pore architecture allow cancer cell entry into or exit from drug-resistant dormancy. *Am. J. Pathol.* **180**, 375-389 (2012).
41. Chow, K.-H., Factor, R. E. & Ullman, K. S. The nuclear envelope environment and its cancer connections. *Nat. Rev. Cancer* **12**, 196-209 (2012).
42. van der Watt, P. J. *et al.* The Karyopherin proteins, Crm1 and Karyopherin beta1, are overexpressed in cervical cancer and are critical for cancer cell survival and proliferation. *Int. J. Cancer* **124**, 1829-1840 (2009).
43. Doherty, J. A. *et al.* ESR1/SYNE1 polymorphism and invasive epithelial ovarian cancer risk: an Ovarian Cancer Association Consortium study. *Cancer Epidemiol. Biomarkers Prev.* **19**, 245-250 (2010).
44. Moss, S. F. *et al.* Decreased and aberrant nuclear lamin expression in gastrointestinal tract neoplasms. *Gut* **45**, 723-9 (1999).
45. Broers, J. L. *et al.* Nuclear A-type lamins are differentially expressed in human lung cancer subtypes. *Am J Pathol* **143**, 211-20 (1993).

46. Hetzer, M. W., Walther, T. C. & Mattaj, I. W. Pushing the envelope: structure, function, and dynamics of the nuclear periphery. *Annu. Rev. Cell Dev. Biol.* **21**, 347-380 (2005).
47. Voeltz, G. K., Rolls, M. M. & Rapoport, T. A. Structural organization of the endoplasmic reticulum. *EMBO Rep.* **3**, 944-950 (2002).
48. D'Angelo, M. A. & Hetzer, M. W. The role of the nuclear envelope in cellular organization. *Cell. Mol. Life Sci.* **63**, 316-332 (2006).
49. Burke, B. & Ellenberg, J. Remodelling the walls of the nucleus. *Nat. Rev. Mol. Cell Biol.* **3**, 487-497 (2002).
50. Ellenberg, J. *et al.* Nuclear membrane dynamics and reassembly in living cells: targeting of an inner nuclear membrane protein in interphase and mitosis. *J. Cell Biol.* **138**, 1193-1206 (1997).
51. Voeltz, G. K., Prinz, W. A., Shibata, Y., Rist, J. M. & Rapoport, T. A. A class of membrane proteins shaping the tubular endoplasmic reticulum. *Cell* **124**, 573-86 (2006).
52. Shibata, Y., Voeltz, G. K. & Rapoport, T. A. Rough sheets and smooth tubules. *Cell* **126**, 435-9 (2006).
53. Pyrpasopoulou, A., Meier, J., Maison, C., Simos, G. & Georgatos, S. D. The lamin B receptor (LBR) provides essential chromatin docking sites at the nuclear envelope. *Embo J* **15**, 7108-19 (1996).
54. Ellenberg, J. & Lippincott-Schwartz, J. Dynamics and mobility of nuclear envelope proteins in interphase and mitotic cells revealed by green fluorescent protein chimeras. *Methods* **19**, 362-72 (1999).
55. Haraguchi, T. *et al.* Live fluorescence imaging reveals early recruitment of emerin, LBR, RanBP2, and Nup153 to reforming functional nuclear envelopes. *J Cell Sci* **113 ( Pt 5)**, 779-94 (2000).
56. Dultz, E. *et al.* Systematic kinetic analysis of mitotic dis- and reassembly of the nuclear pore in living cells. *J Cell Biol* **180**, 857-65 (2008).
57. Antonin, W., Ellenberg, J. & Dultz, E. Nuclear pore complex assembly through the cell cycle: regulation and membrane organization. *FEBS Lett* **582**, 2004-16 (2008).

58. Gant, T. M., Harris, C. A. & Wilson, K. L. Roles of LAP2 proteins in nuclear assembly and DNA replication: truncated LAP2beta proteins alter lamina assembly, envelope formation, nuclear size, and DNA replication efficiency in *Xenopus laevis* extracts. *J Cell Biol* **144**, 1083-96 (1999).
59. Holmer, L. & Worman, H. J. Inner nuclear membrane proteins: functions and targeting. *Cell Mol Life Sci* **58**, 1741-7 (2001).
60. Foisner, R. Cell cycle dynamics of the nuclear envelope. *TheScientificWorldJournal* **3**, 1-20 (2003).
61. Liu, J. *et al.* MAN1 and emerin have overlapping function(s) essential for chromosome segregation and cell division in *Caenorhabditis elegans*. *Proc Natl Acad Sci U S A* **100**, 4598-603 (2003).
62. Walther, T. C. *et al.* The conserved Nup107-160 complex is critical for nuclear pore complex assembly. *Cell* **113**, 195-206 (2003).
63. Ye, Q. & Worman, H. J. Interaction between an integral protein of the nuclear envelope inner membrane and human chromodomain proteins homologous to *Drosophila* HP1. *J Biol Chem* **271**, 14653-6 (1996).
64. Furukawa, K., Fritze, C. E. & Gerace, L. The major nuclear envelope targeting domain of LAP2 coincides with its lamin binding region but is distinct from its chromatin interaction domain. *J Biol Chem* **273**, 4213-9 (1998).
65. Segura-Totten, M., Kowalski, A. K., Craigie, R. & Wilson, K. L. Barrier-to-autointegration factor: major roles in chromatin decondensation and nuclear assembly. *J Cell Biol* **158**, 475-85 (2002).
66. Gorjanacz, M. *et al.* *Caenorhabditis elegans* BAF-1 and its kinase VRK-1 participate directly in post-mitotic nuclear envelope assembly. *Embo J* **26**, 132-43 (2007).
67. Haraguchi, T. *et al.* Live cell imaging and electron microscopy reveal dynamic processes of BAF-directed nuclear envelope assembly. *J Cell Sci* **121**, 2540-54 (2008).
68. Ulbert, S., Platani, M., Boue, S. & Mattaj, I. W. Direct membrane protein-DNA interactions required early in nuclear envelope assembly. *J Cell Biol* **173**, 469-76 (2006).

69. Mansfeld, J. *et al.* The conserved transmembrane nucleoporin NDC1 is required for nuclear pore complex assembly in vertebrate cells. *Mol Cell* **22**, 93-103 (2006).
70. Stavru, F. *et al.* NDC1: a crucial membrane-integral nucleoporin of metazoan nuclear pore complexes. *J Cell Biol* **173**, 509-19 (2006).
71. Ketema, M. *et al.* Requirements for the localization of nesprin-3 at the nuclear envelope and its interaction with plectin. *J Cell Sci* **120**, 3384-94 (2007).
72. Somech, R. *et al.* Enhanced expression of the nuclear envelope LAP2 transcriptional repressors in normal and malignant activated lymphocytes. *Ann Hematol* **86**, 393-401 (2007).
73. Zink, D., Fischer, A. H. & Nickerson, J. A. Nuclear structure in cancer cells. *Nat Rev Cancer* **4**, 677-87 (2004).
74. Fischer, A. H. *et al.* The cytologic criteria of malignancy. *J Cell Biochem* **110**, 795-811 (2010).
75. Broers, J. L. *et al.* Decreased mechanical stiffness in LMNA<sup>-/-</sup> cells is caused by defective nucleo-cytoskeletal integrity: implications for the development of laminopathies. *Hum Mol Genet* **13**, 2567-80 (2004).
76. Lammerding, J. *et al.* Lamin A/C deficiency causes defective nuclear mechanics and mechanotransduction. *J Clin Invest* **113**, 370-8 (2004).
77. Newport, J. W., Wilson, K. L. & Dunphy, W. G. A lamin-independent pathway for nuclear envelope assembly. *J Cell Biol* **111**, 2247-59 (1990).
78. Lammerding, J. *et al.* Lamins A and C but not lamin B1 regulate nuclear mechanics. *J Biol Chem* **281**, 25768-80 (2006).
79. Dittmer, T. A. & Misteli, T. The lamin protein family. *Genome Biol* **12**, 222 (2011).
80. Vergnes, L., Peterfy, M., Bergo, M. O., Young, S. G. & Reue, K. Lamin B1 is required for mouse development and nuclear integrity. *Proc Natl Acad Sci U S A* **101**, 10428-33 (2004).

81. Sullivan, T. *et al.* Loss of A-type lamin expression compromises nuclear envelope integrity leading to muscular dystrophy. *J Cell Biol* **147**, 913-20 (1999).
82. Lee, J. S. *et al.* Nuclear lamin A/C deficiency induces defects in cell mechanics, polarization, and migration. *Biophys J* **93**, 2542-52 (2007).
83. Raharjo, W. H., Enarson, P., Sullivan, T., Stewart, C. L. & Burke, B. Nuclear envelope defects associated with LMNA mutations cause dilated cardiomyopathy and Emery-Dreifuss muscular dystrophy. *J Cell Sci* **114**, 4447-57 (2001).
84. Burke, B. & Stewart, C. L. The laminopathies: the functional architecture of the nucleus and its contribution to disease. *Annu Rev Genomics Hum Genet* **7**, 369-405 (2006).
85. Margalit, A., Vlack, S., Gruenbaum, Y. & Foisner, R. Breaking and making of the nuclear envelope. *Journal of cellular biochemistry* **95**, 454-65 (2005).
86. Hetzer, M. W. The nuclear envelope. *Cold Spring Harb Perspect Biol* **2**, a000539 (2010).
87. Anderson, D. J., Vargas, J. D., Hsiao, J. P. & Hetzer, M. W. Recruitment of functionally distinct membrane proteins to chromatin mediates nuclear envelope formation in vivo. *J. Cell Biol.* **186**, 183-191 (2009).
88. Gerace, L. & Foisner, R. Integral membrane proteins and dynamic organization of the nuclear envelope. *Trends in cell biology* **4**, 127-31 (1994).
89. De Vos, W. H. *et al.* Repetitive Disruptions of the Nuclear Envelope Invoke Temporary Loss of Cellular Compartmentalization in Laminopathies. *Hum Mol Genet* (2011).doi:ddr344 [pii] 10.1093/hmg/ddr344
90. Venables, R. S. *et al.* Expression of individual lamins in basal cell carcinomas of the skin. *Br J Cancer* **84**, 512-9 (2001).
91. Machiels, B. M. *et al.* Abnormal A-type lamin organization in a human lung carcinoma cell line. *Eur J Cell Biol* **67**, 328-35 (1995).

92. Jansen, M. P. *et al.* Comparison of A and B-type lamin expression in reactive lymph nodes and nodular sclerosing Hodgkin's disease. *Histopathology* **31**, 304-12 (1997).
93. Marme, A. *et al.* Loss of Drop1 expression already at early tumor stages in a wide range of human carcinomas. *Int J Cancer* **123**, 2048-56 (2008).
94. Kaufmann, S. H. Expression of nuclear envelope lamins A and C in human myeloid leukemias. *Cancer Res* **52**, 2847-53 (1992).
95. Kaufmann, S. H., Mabry, M., Jasti, R. & Shaper, J. H. Differential expression of nuclear envelope lamins A and C in human lung cancer cell lines. *Cancer Res* **51**, 581-6 (1991).
96. Capo-Chichi, C. D. *et al.* Loss of A-type lamin expression compromises nuclear envelope integrity in breast cancer. *Chin J Cancer* **30**, 415-25 (2011).
97. de Noronha, C. M. *et al.* Dynamic disruptions in nuclear envelope architecture and integrity induced by HIV-1 Vpr. *Science* **294**, 1105-8 (2001).
98. De Vos, W. H. *et al.* Increased plasticity of the nuclear envelope and hypermobility of telomeres due to the loss of A-type lamins. *Biochimica et biophysica acta* **1800**, 448-58 (2010).
99. Dechat, T. *et al.* Nuclear lamins: major factors in the structural organization and function of the nucleus and chromatin. *Genes & Development* **22**, 832-853 (2008).
100. Stewart, C. L., Roux, K. J. & Burke, B. Blurring the boundary: the nuclear envelope extends its reach. *Science* **318**, 1408-12 (2007).
101. Shimi, T. *et al.* The A- and B-type nuclear lamin networks: microdomains involved in chromatin organization and transcription. *Genes Dev* **22**, 3409-21 (2008).
102. Coffinier, C. *et al.* Abnormal development of the cerebral cortex and cerebellum in the setting of lamin B2 deficiency. *Proc Natl Acad Sci U S A* **107**, 5076-81 (2010).
103. Le Hir, H. & Andersen, G. R. Structural insights into the exon junction complex. *Current opinion in structural biology* **18**, 112-9 (2008).

104. Chang, Y. F., Imam, J. S. & Wilkinson, M. F. The nonsense-mediated decay RNA surveillance pathway. *Annual review of biochemistry* **76**, 51-74 (2007).
105. Foisner, R. & Gerace, L. Integral membrane proteins of the nuclear envelope interact with lamins and chromosomes, and binding is modulated by mitotic phosphorylation. *Cell* **73**, 1267-79 (1993).
106. Kau, T. R., Way, J. C. & Silver, P. A. Nuclear transport and cancer: from mechanism to intervention. *Nature reviews. Cancer* **4**, 106-17 (2004).
107. Bernhard, W. & Granboulan, N. The Fine Structure of the Cancer Cell Nucleus. *Experimental cell research* **24**, SUPPL9:19-53 (1963).
108. Brandes, D., Schofield, B. H. & Anton, E. Nuclear mitochondria? *Science* **149**, 1373-4 (1965).
109. Muller, P. R. *et al.* Nuclear lamin expression reveals a surprisingly high growth fraction in childhood acute lymphoblastic leukemia cells. *Leukemia : official journal of the Leukemia Society of America, Leukemia Research Fund, U.K* **8**, 940-5 (1994).
110. Collard, J. F., Senecal, J. L. & Raymond, Y. Redistribution of nuclear lamin A is an early event associated with differentiation of human promyelocytic leukemia HL-60 cells. *Journal of cell science* **101 ( Pt 3)**, 657-70 (1992).
111. Stadelmann, B. *et al.* Repression of nuclear lamin A and C gene expression in human acute lymphoblastic leukemia and non-Hodgkin's lymphoma cells. *Leukemia research* **14**, 815-21 (1990).
112. Belt, E. J. *et al.* Loss of lamin A/C expression in stage II and III colon cancer is associated with disease recurrence. *European journal of cancer* **47**, 1837-45 (2011).
113. Skvortsov, S. *et al.* Proteomics profiling of microdissected low- and high-grade prostate tumors identifies Lamin A as a discriminatory biomarker. *Journal of proteome research* **10**, 259-68 (2011).
114. Heddle, J. A. & Carrano, A. V. The DNA content of micronuclei induced in mouse bone marrow by gamma-irradiation: evidence that micronuclei arise from acentric chromosomal fragments. *Mutation research* **44**, 63-9 (1977).

115. Heddle, J. A. *et al.* The induction of micronuclei as a measure of genotoxicity. A report of the U.S. Environmental Protection Agency Gene-Tox Program. *Mutation research* **123**, 61-118 (1983).
116. Shimizu, N., Kanda, T. & Wahl, G. M. Selective capture of acentric fragments by micronuclei provides a rapid method for purifying extrachromosomally amplified DNA. *Nature genetics* **12**, 65-71 (1996).
117. Gilula, N. B., Epstein, M. L. & Beers, W. H. Cell-to-cell communication and ovulation. A study of the cumulus-oocyte complex. *J. Cell Biol.* **78**, 58-75 (1978).